ECOSYSTEM-BASED FISHERIES MANAGEMENT THRESHOLDS FOR HAWAI'I NEARSHORE FISHERIES

FINAL REPORT

SEPTEMBER 2022

Project Team: Shannon Hennessey[1,2], Jamison Gove[3,4], Mary Donovan[1,2]

[1]School of Geographical Sciences and Urban Planning, Center for Global Discovery and Conservation Science, Arizona State University
[2]Hawai'i Monitoring and Reporting Collaborative
[3]Ecosystem Sciences Division, Pacific Islands Fisheries Science Center, National Oceanic and Atmospheric Administration
[4]Hawai'i Integrated Ecosystem Assessment Program, Pacific Islands Fisheries Science Center, National Oceanic and Atmospheric Administration

Principal Investigator: Mary Donovan, Arizona State University, marydonovan@asu.edu

EXECUTIVE SUMMARY

Purpose And Background

The National Oceanic and Atmospheric Administration's (NOAA) National Marine Fisheries Service (NMFS) has increasingly moved towards ecosystem-based fisheries management (EBFM). Updates to the Magnuson-Stevens Fishery Conservation and Management Act in 1996 and 2007 included directions for Fishery Management Councils to assess ecosystem considerations, leading to the development of Fishery Ecosystem Plans. NOAA has also developed the Integrated Ecosystem Assessment (IEA) program to conduct and provide ecosystem-science to natural resource management. Central to this process is providing scientific support for questions related to EBFM concepts, including the development of indicators. Indicators play a role in assessment and monitoring of ecosystem state by relating ecological and social outcomes with management goals in the form of threshold levels of environmental and human drivers. A threshold can be defined as the point at which there is a rapid, non-linear change in the ecosystem in response to a driver, with the potential to indicate whether an ecosystem is moving between a desired state and an undesired state.

For example, the Pacific Fisheries Management Council (PFMC) has been implementing an indicator approach to ecosystem management for the U.S. California Current Ecosystem (CCE) since 2012, and the California Current Integrated Ecosystem Assessment program (CCIEA) has been providing annual indicator updates to the Council since 2015. PFMC uses these indicators to inform fishery managers about the state of the environment upon which stocks and fisheries operate to make management decisions with ecosystem considerations. Recent frameworks developed in the CCE and elsewhere for developing ecosystem indicators are based on potential non-linear responses (thresholds) to environmental and human pressures.

In the Pacific, nearshore reefs are complex ecosystems, with multiple interacting drivers that vary in space and time, therefore applying EBFM principles is particularly relevant in this area. However, more information is needed on the spatial and temporal context of relationships between ecological indicators and environmental and human pressures, especially in the context of ongoing management needs. Specifically, to move beyond single-species assessments there is a need to understand the utility of species complexes as indicators, especially given that available fisheries-dependent data is generally collected for species complexes.

We undertook a pilot study to explore the utility of EBFM indicator approaches for Pacific fisheries. We began with an initial focus on nearshore species in Hawai‘i owing to the availability of existing data to answer our questions. **The major questions that we addressed were:**

- Is there evidence for threshold relationships between fisheries indicators and environmental drivers in nearshore ecosystems of Hawai‘i?
- Are there commonalities in the thresholds across species and their functional and family groups?

Summary of Project Approach

We followed a framework established by the NOAA Integrated Ecosystem Assessment program that draws on multiple statistical methods and provides four steps for defining the relationship between an ecosystem indicator and pressure (Samhouri et al. 2017).

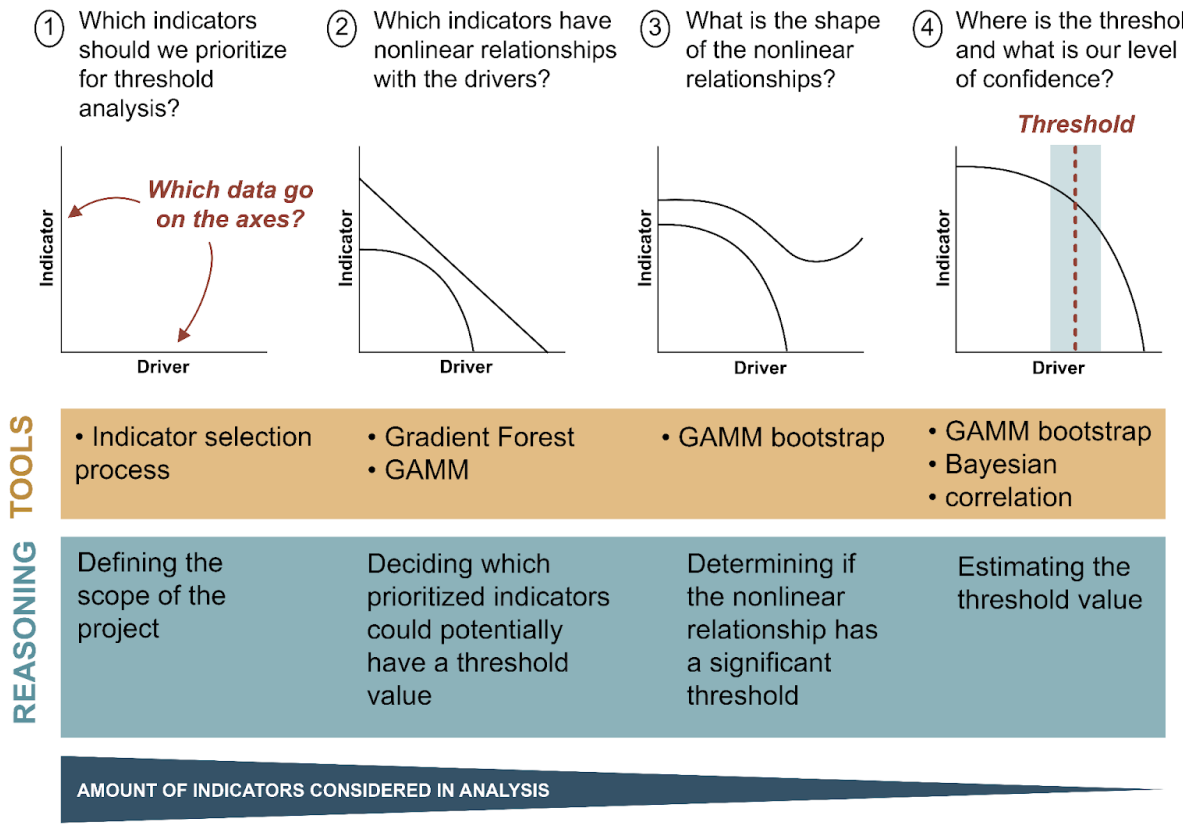

Graphical representation of steps used in project approach. We followed four major steps to identify potential thresholds between ecosystem indicators and drivers based on methods established by Samhouri et al. (2017).

Step 1: Which data?

The first step was to define which variables were considered in the analyses, including both indicators (y-axis) and drivers (x-axis).

We prioritized indicators relevant to nearshore fisheries in Hawai‘i, using previously identified priority species from the Hawai‘i Coral Reef Strategy, and by reviewing existing sources to identify species dominant in available landings data. We then included family and functional groups for each species to assess utility for basing management targets on aggregated species complexes. Data for the indicators were from an existing compilation of fisheries independent underwater visual census data, including over 5,000 observations.

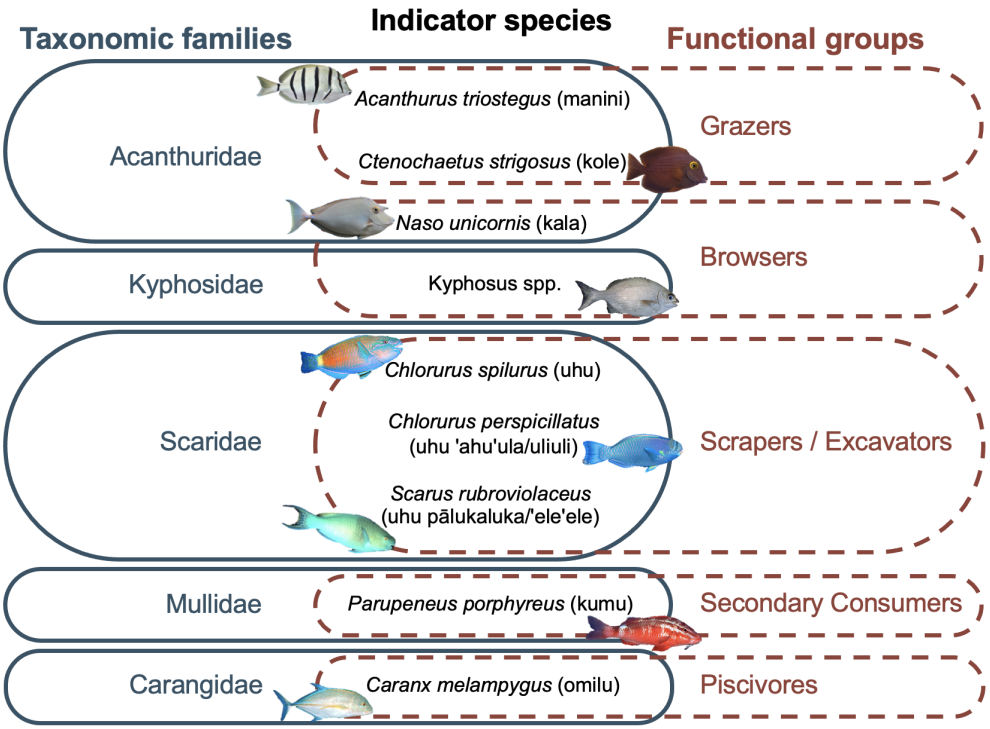

Species used in the analyses and their associated taxonomic families and ecological functional groups. Ovals show where families and functional groups overlap.

We then paired indicators with driver variables with a focus on environmental (oceanographic and habitat) variables to establish an understanding of the fundamental relationships between the ecological indicators and the natural system. Environmental driver data relied heavily on previous work to develop fine-resolution modeled and satellite-based metrics of four environmental drivers for Hawai‘i including: sea surface temperature, chlorophyll-a, irradiance, and wave forcing.

Step 2: Are there nonlinearities?

We used multi-model inference to identify significant nonlinear relationships by incorporating multiple statistical methods to define the relationship between an ecosystem indicator and driver. This included gradient forest, a modeling framework that provides the ability to consider multiple indicators together along a gradient of a given environmental driver. The second modeling framework we used was Generalized Additive Mixed Models (GAMMs), which fit statistically robust and flexible relationships to the data while accounting for spatial and temporal variation. Together, these two modeling frameworks complement each other in their ability to robustly identify complex relationships.

Gradient forests identified four drivers that had evidence for threshold relationships with one or more indicators. Those were:

1) depth
2) habitat complexity
3) wave anomaly frequency
4) wave anomaly magnitude

We then used generalized additive mixed models (GAMMs) to investigate each indicator-driver relationship in more detail, fitting 2 different models to each indicator-driver pair: (1) a binomial response based on presence-absence data, and (2) a gamma response based on biomass data where the indicator was present. All models included the random effects of dataset, island, and habitat type.

Of 380 candidate GAMM models, 81 met nonlinearity significance criteria. Of those, 13 significant nonlinear indicator–driver pairs were also supported by gradient forest analysis. These 13 combinations of indicators and drivers were the focus of the subsequent analyses.

Steps 3 and 4: What type of nonlinearity exists, and how strong are the nonlinearities?

With 13 significantly nonlinear pairs identified, we determined whether each nonlinear relationship had a significant threshold. To do this, we used the previously fitted GAMM models, and bootstrapped the fits to estimate a 95% confidence interval for the fitted function. We also calculated the second derivative of each bootstrapped fit to also estimate where along the driver the 95% interval of the second derivative crossed zero. This provided evidence for what range of the driver a potential threshold might lie within.

We then defined a threshold point estimate as our 'best estimate' of the threshold as the driver values where the 2nd derivative is at a minimum or maximum along the threshold range.

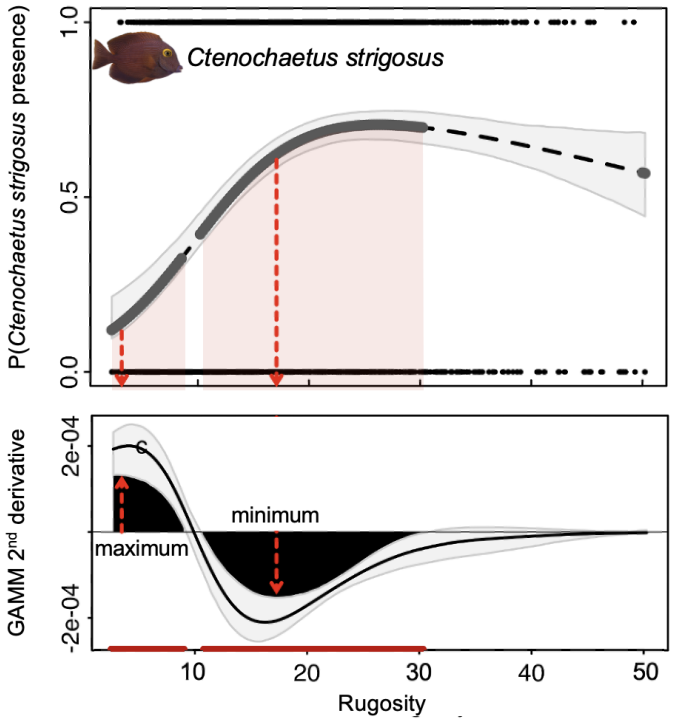

Example of non-linear fit (top) between an ecosystem indicator (y-axis, probability of *Ctenochaetus strigosus* presence) and driver (x-axis, rugosity (habitat complexity)), with threshold ranges (gray lines and red polygons) identified from regions where 95% intervals of bootstrapped second derivative estimates (bottom) did not overlap zero (black polygons). Red dashed lines are the point estimates of threshold locations corresponding to the minimum or maximum of the second derivative.

Significant thresholds were identified for

- 3 species: *Naso unicornis* (kala), *Ctenochaetus strigosus* (kole), and *Chlorurus spilurus* (uhu),
- 2 families: Acanthuridae and Kyphosidae,
- and 1 functional group, browsers.

Across the 4 environmental drivers:

- depth,
- rugosity,
- wave anomaly maximum, and
- wave anomaly frequency.

Conclusions and applications to management

We provided a step forward in the development of science that can support implementation of EBFM by exploring the potential for thresholds to be estimated for ecosystem indicators of Hawai‘i nearshore fisheries. Indicators can be useful for ecosystem-based approaches when they capture complex and dynamic ecosystem responses. We explored this utility by investigating whether there was evidence for commonalities in thresholds across species and their functional and family groups represented in nearshore fisheries in Hawai‘i. We found evidence for thresholds across four environmental drivers and multiple indicators, with some commonalities apparent, especially for habitat complexity (rugosity) and wave forcing. This represents a first step in assessing the utility of an indicator approach to EBFM for Pacific nearshore ecosystems.

We identified both strengths and weaknesses of our approach lending to several possible next steps for moving forward science to support EBFM implementation. Given this, more work is needed to meet the broader objective *to provide a quantitative basis for ecosystem management that can be used to design effective management targets and measure and evaluate actions once they are in place*. That said, this work relates to the following management implications:

- Given that many of the species that comprise nearshore fisheries in the Pacific are data poor, and when fisheries dependent data are collected they are often collected at the species complex level (e.g., all uhu combined in Hawai‘i), the commonalities and differences we identified across species and species complexes has implications for how they are monitored for EBFM.
- In addition to screening potential indicators and drivers for further analyses, this work also emphasizes the role of variation in environmental controls. Understanding the limits of their control on ecosystem responses can provide a basis for monitoring and decision making.
- Our analyses focused on environmental drivers rather than those associated with humans (fishing, land-based pollution) due to the importance of first understanding the role of environmental variation on indicators. Thus, future work can build on these to understand how humans alter those fundamental relationships.

ECOSYSTEM-BASED FISHERIES MANAGEMENT THRESHOLDS FOR HAWAI'I NEARSHORE FISHERIES

Shannon Hennessey[1,2], Jamison Gove[3,4], Mary Donovan[1,2]

[1] School of Geographical Sciences and Urban Planning, Center for Global Discovery and Conservation Science, Arizona State University
[2] Hawai'i Monitoring and Reporting Collaborative
[3] Ecosystem Sciences Division, Pacific Islands Fisheries Science Center, National Oceanic and Atmospheric Administration
[4] Hawai'i Integrated Ecosystem Assessment Program, Pacific Islands Fisheries Science Center, National Oceanic and Atmospheric Administration

Indicators as a Tool for Ecosystem-Based Fisheries Management

Ecosystem-Based Fisheries Management (EBFM) has been recognized as a management priority throughout the world (Arkema et al. 2006, Crowder and Norse 2008, Levin and Lubchenco 2008, Levin et al. 2009, Mcleod and Leslie 2009). EBFM recognizes that ecosystems are dynamic with components that can have integrated responses to interacting drivers, especially when human impacts accumulate in time and space and management trade-offs are needed to optimize multiple outcomes.

In the United States, NOAA mandates have increasingly moved towards ecosystem approaches. In particular, the Magnuson-Stevens Fishery Conservation and Management Act updates in 1996 and 2007 included directions for Fishery Management Councils to assess ecosystem considerations, leading to the development of Fishery Ecosystem Plans (Dolan et al. 2015). NOAA has also developed the Integrated Ecosystem Assessment (IEA) program for providing a vehicle to conduct and deliver ecosystem-science to management (Levin et al. 2009, Samhouri et al. 2013, Harvey et al. 2016). Central to this process is providing scientific support for questions related to EBFM concepts such as cumulative impacts (Halpern et al. 2009), management trade-offs (White et al. 2012, Lester et al. 2013), and ecosystem indicators (Link 2005, Methratta and Link 2006, Samhouri et al. 2009). Indicators can relate ecological and social outcomes with management goals in the form of threshold levels of environmental and human drivers (Samhouri et al. 2013, Boldt et al. 2014) (Figure 1).

For example, the Pacific Fisheries Management Council (PFMC) has been implementing an indicator approach to ecosystem management for the U.S. California Current Ecosystem (CCE) since 2012, and the California Current Integrated Ecosystem Assessment program (CCIEA) has been providing annual indicator updates to the Council since 2015. PFMC uses these indicators to inform fishery managers about the state of the environment upon which stocks and fisheries operate to make fishery management decisions with ecosystem considerations. Knowing the state of the environment allows management to adjust their conservation measures based on

the productivity level of the stocks in response to the changing environment. Indicators for the CCE are focused on ecosystem states and environmental and human pressures analyzed in reference to long-term average conditions (*The California Current Integrated Ecosystem Assessment: Phase III Report* 2014). Further, recent frameworks developed in the CCE and elsewhere for developing ecosystem indicators are based on potential non-linear responses (thresholds) to environmental and human pressures (Samhouri et al. 2010, Large et al. 2013, Foley et al. 2015, Selkoe et al. 2015) (Figure 1). Common nonlinear responses to pressures have also been identified across four large-marine ecosystems in the United States (Tam et al. 2017). Together, these examples provide a path forward for implementing an indicator approach to ecosystem-based management (Foley et al. 2013, Selkoe et al. 2015).

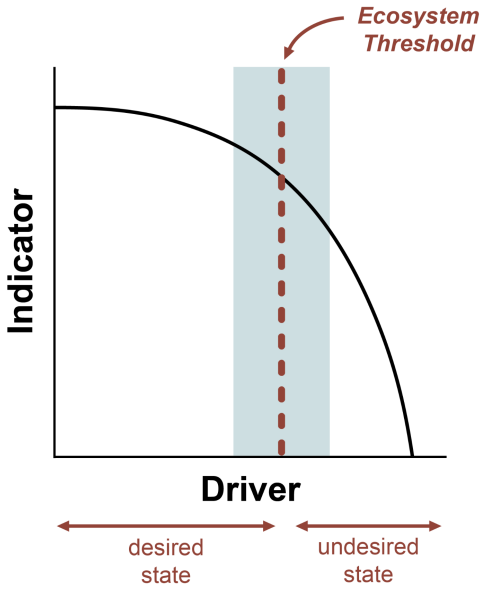

Figure 1. Framework for applying the concept of thresholds to analysis of ecological indicators. The indicator of ecosystem status is modeled as a function of the driver, and a threshold between the two can be used to establish an ecosystem threshold. When the driver is below the threshold the ecosystem may be in a desired state compared to an undesired state when the driver is above the threshold. Modified from Selkoe et al (2015).

In Hawai‘i, efforts to implement EBFM are underway with parallel science needs from the Western Pacific Fisheries Management Council’s Hawai‘i Fishery Ecosystem Plan, the Hawai‘i Integrated Ecosystem Assessment Program, and the State of Hawai‘i’s nearshore management. Each of these efforts relies on assessments of the status and trends of Hawai‘i’s coral reef ecosystems, and tools to evaluate the response of the ecosystems to management. Environmental pressures are known to be important drivers of ecosystem state in Hawai‘i (Dollar 1982, Grigg 1998, Dollar and Grigg 2004, Gove et al. 2013), and relationships to human activities are also well documented (Friedlander and DeMartini 2002, Friedlander et al. 2003, Jokiel et al. 2004, Williams et al. 2008, Jouffray et al. 2019). However, more information is needed on the spatial and temporal context of relationships between ecological indicators and environmental and human pressures, especially in the context of ongoing management needs.

To address needs for science to inform EBFM in Hawai‘i, we have conducted analyses to address several knowledge gaps. Available fisheries data for nearshore areas in Hawai‘i are most frequently reported at either a species, or more commonly, the species-complex level. For example, commercial fisheries for parrotfishes are reported for all species combined, despite

large differences in life histories between several large-bodied species and small-bodied species (DeMartini and Howard 2016). To move beyond single-species assessments, and also to test the utility of species complexes as indicators, we investigated the relationships between individual species, functional groups, and families with environmental drivers. With these comparisons we were able to address the following questions:

1. Is there evidence for threshold relationships between fisheries indicators and drivers in nearshore ecosystems of Hawai‘i?
2. Are there commonalities in the thresholds across species and their functional and family groups?

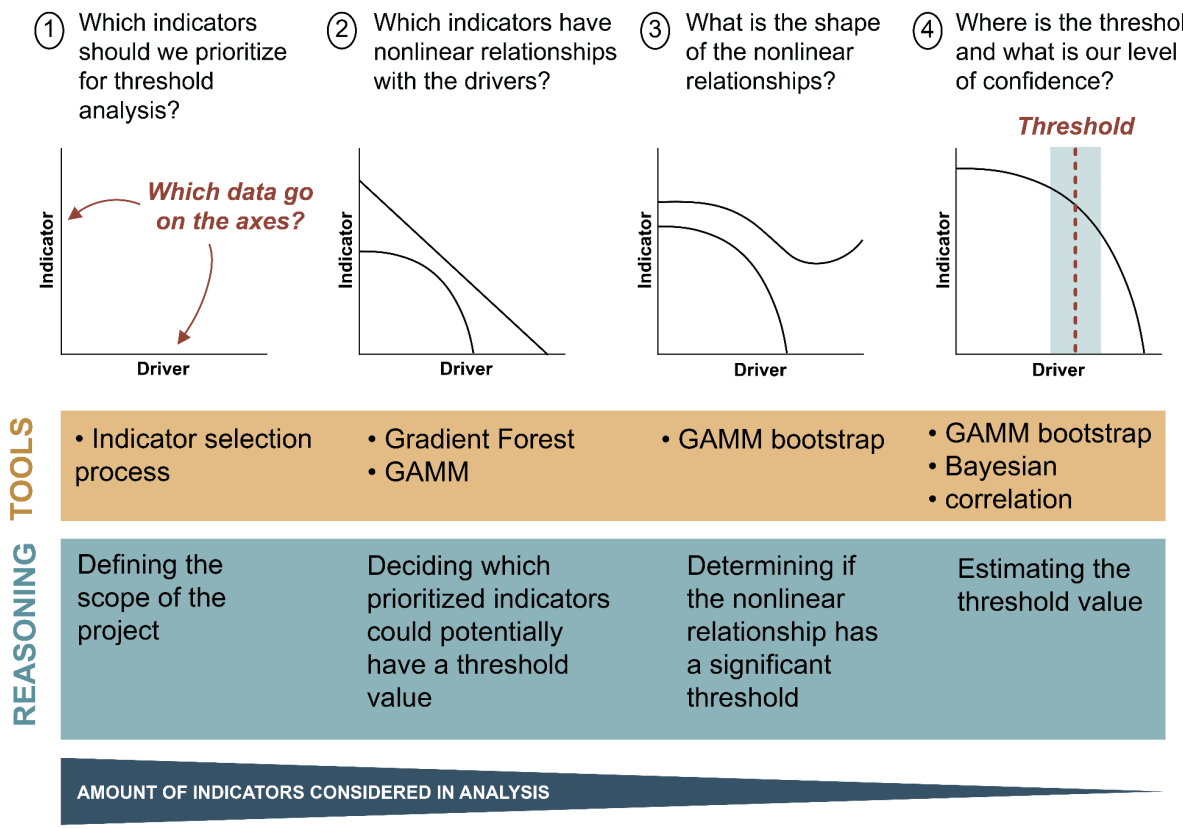

Figure 2. Graphical representation of steps used in project approach. We followed four major steps to identify potential thresholds between ecosystem indicators and drivers based on methods established by Samhouri et al. (2017).

To identify thresholds in our indicator and ecosystem driver relationships in Hawai‘i nearshore reef ecosystems, we followed several steps involving multiple quantitative tools (Figure 2):

1) identify which indicators and drivers should be prioritized for analysis,
2) screen indicator-driver relationships for non-linearities,
3) identify the shape of non-linear relationships,
4) estimate thresholds and confidence intervals around those thresholds.

Clarifying focus and identifying data

To first understand which species and species complexes were important for Hawai‘i nearshore reef fisheries, we reviewed data from existing fisheries reporting (Table 1).

Table 1. Hawai‘i nearshore species and species complexes as included in existing fisheries reporting or analyses. **Bolded** species and species complexes indicate groups used in our analyses. A (*) indicates a species identified as a priority by the Fisheries Local Action Strategy in Hawai‘i (FLASH). DLNR-DAR: Hawaii Division of Aquatic Resources; CML: Commercial Marine Landings Database; WPRFMC Hawaii FEP: Western Pacific Fisheries Management Council Fisheries Ecosystem Plan. (Nadon et al. 2015) includes species that were assessed with length-based stock assessments, and (McCoy et al. 2018) includes species that were reported by the Marine Recreational Information Program (MRIP).

Indicator	Species	References
Acanthuridae	*Acanthurus achilles*	DLNR-DAR CML 2004-2013; McCoy et al 2018
	Acanthurus blochii	DLNR-DAR CML 2004-2013; WPRFMC Hawaii FEP 2009; Nadon et al. 2015; McCoy et al 2018
	Acanthurus dussumieri	DLNR-DAR CML 2004-2013; WPRFMC Hawaii FEP 2009; Nadon et al. 2015; McCoy et al 2018
	Acanthurus guttatus	WPRFMC Hawaii FEP 2009
	Acanthurus leucopareius	WPRFMC Hawaii FEP 2009; McCoy et al 2018
	Acanthurus nigroris	DLNR-DAR CML 2004-2013; WPRFMC Hawaii FEP 2009; McCoy et al 2018
	Acanthurus olivaceus	WPRFMC Hawaii FEP 2009; McCoy et al 2018
	Acanthurus triostegus*	DLNR-DAR CML 2004-2013; WPRFMC Hawaii FEP 2009; McCoy et al 2018
	Acanthurus xanthopterus	WPRFMC Hawaii FEP 2009; McCoy et al 2018
	Ctenochaetus hawaiiensis	DLNR-DAR CML 2004-2013; McCoy et al 2018
	Ctenochaetus strigosus*	DLNR-DAR CML 2004-2013; WPRFMC Hawaii FEP 2009; McCoy et al 2018
	Naso annulatus	WPRFMC Hawaii FEP 2009; McCoy et al 2018
	Naso brevirostris	WPRFMC Hawaii FEP 2009; Nadon et al. 2015; McCoy et al 2018
	Naso caesius	WPRFMC Hawaii FEP 2009
	Naso hexacanthus	DLNR-DAR CML 2004-2013; WPRFMC Hawaii FEP 2009; Nadon et al. 2015; McCoy et al 2018
	Naso lituratus	DLNR-DAR CML 2004-2013; WPRFMC Hawaii FEP 2009; Nadon et al. 2015; McCoy et al 2018
	Naso unicornis*	WPRFMC Hawaii FEP 2009; McCoy et al 2018
Carangidae	*Alectis ciliaris*	DLNR-DAR CML 2004-2013; McCoy et al 2018
	Carangoides ferdau	McCoy et al 2018
	Carangoides orthogrammus	DLNR-DAR CML 2004-2013; Nadon et al. 2015; McCoy et al 2018
	*Caranx ignobilis**	DLNR-DAR CML 2004-2013; Nadon et al. 2015; McCoy et al 2018
	Caranx lugubris	McCoy et al 2018
	Caranx melampygus*	DLNR-DAR CML 2004-2013; Nadon et al. 2015; McCoy et al 2018
	Caranx sexfasciatus	DLNR-DAR CML 2004-2013; McCoy et al 2018
	Gnathanodon speciosus	DLNR-DAR CML 2004-2013; McCoy et al 2018
	Scomberoides lysan	DLNR-DAR CML 2004-2013; McCoy et al 2018
	Seriola dumerili	DLNR-DAR CML 2004-2013; McCoy et al 2018
Holocentridae	*Myripristis amaena*	WPRFMC Hawaii FEP 2009; McCoy et al 2018
	Myripristis berndti	WPRFMC Hawaii FEP 2009; Nadon et al. 2015; McCoy et al 2018

	Myripristis chryseres	WPRFMC Hawaii FEP 2009; McCoy et al 2018
	Myripristis kuntee	WPRFMC Hawaii FEP 2009
	Myripristis vittata	McCoy et al 2018
	Sargocentron punctatissimum	WPRFMC Hawaii FEP 2009
	Sargocentron spiniferum	DLNR-DAR CML 2004-2013; WPRFMC Hawaii FEP 2009; McCoy et al 2018
	Sargocentron tiere	DLNR-DAR CML 2004-2013; WPRFMC Hawaii FEP 2009; McCoy et al 2018
	Sargocentron xantherythrum	WPRFMC Hawaii FEP 2009; McCoy et al 2018
Kuhliidae	*Kuhlia sandvicensis*	WPRFMC Hawaii FEP 2009
Kyphosidae	*Kyphosus bigibbus**	McCoy et al 2018
	*Kyphosus cinerascens**	WPRFMC Hawaii FEP 2009; McCoy et al 2018
	*Kyphosus vaigiensis**	WPRFMC Hawaii FEP 2009; McCoy et al 2018
Labridae	*Anampses cuvier*	McCoy et al 2018
	Bodianus albotaeniatus	WPRFMC Hawaii FEP 2009
	Coris flavovittata	McCoy et al 2018
	Iniistius baldwini	McCoy et al 2018
	Iniistius pavo	WPRFMC Hawaii FEP 2009; McCoy et al 2018
	Iniistius umbrilatus	McCoy et al 2018
	Oxycheilinus unifasciatus	DLNR-DAR CML 2004-2013; WPRFMC Hawaii FEP 2009; McCoy et al 2018
	Thalassoma ballieui	McCoy et al 2018
	Thalassoma purpureum	WPRFMC Hawaii FEP 2009
Lethrinidae	*Monotaxis grandoculis*	DLNR-DAR CML 2004-2013; Nadon et al. 2015; McCoy et al 2018
Lutjanidae	*Aphareus furca*	DLNR-DAR CML 2004-2013; McCoy et al 2018
	Aprion virescens	Nadon et al. 2015; McCoy et al 2018
	Lutjanus fulvus	DLNR-DAR CML 2004-2013; Nadon et al. 2015; McCoy et al 2018
	Lutjanus kasmira	DLNR-DAR CML 2004-2013; Nadon et al. 2015; McCoy et al 2018
Mugilidae	*Mugil cephalus*	WPRFMC Hawaii FEP 2009; McCoy et al 2018
	Neomyxus leuciscus	WPRFMC Hawaii FEP 2009; McCoy et al 2018
Mullidae	*Mulloidichthys flavolineatus*	DLNR-DAR CML 2004-2013; WPRFMC Hawaii FEP 2009; Nadon et al. 2015; McCoy et al 2018
	Mulloidichthys pfluegeri	WPRFMC Hawaii FEP 2009; Nadon et al. 2015; McCoy et al 2018
	Mulloidichthys vanicolensis	DLNR-DAR CML 2004-2013; WPRFMC Hawaii FEP 2009; Nadon et al. 2015; McCoy et al 2018
	Parupeneus cyclostomus	DLNR-DAR CML 2004-2013; WPRFMC Hawaii FEP 2009; Nadon et al. 2015; McCoy et al 2018
	Parupeneus insularis	DLNR-DAR CML 2004-2013; Nadon et al. 2015; McCoy et al 2018
	Parupeneus multifasciatus	DLNR-DAR CML 2004-2013; WPRFMC Hawaii FEP 2009; McCoy et al 2018
	Parupeneus pleurostigma	DLNR-DAR CML 2004-2013; WPRFMC Hawaii FEP 2009; McCoy et al 2018
	Parupeneus porphyreus*	DLNR-DAR CML 2004-2013; Nadon et al. 2015; McCoy et al 2018
	Upeneus taeniopterus	WPRFMC Hawaii FEP 2009
Pomacentridae	*Abudefduf abdominalis*	DLNR-DAR CML 2004-2013; McCoy et al 2018
Priacanthidae	*Heteropriacanthus cruentatus*	WPRFMC Hawaii FEP 2009; McCoy et al 2018
	Priacanthus meeki	McCoy et al 2018
Scaridae	*Calotomus carolinus*	DLNR-DAR CML 2004-2013; WPRFMC Hawaii FEP 2009; McCoy et al 2018
	Chlorurus perspicillatus*	WPRFMC Hawaii FEP 2009; McCoy et al 2018
	Chlorurus spilurus*	WPRFMC Hawaii FEP 2009

	Scarus dubius	WPRFMC Hawaii FEP 2009; McCoy et al 2018
	Scarus psittacus	WPRFMC Hawaii FEP 2009; McCoy et al 2018
	Scarus rubroviolaceus*	WPRFMC Hawaii FEP 2009; McCoy et al 2018
Serranidae	*Cephalopholis argus*	Nadon et al. 2015; McCoy et al 2018
Sphyraenidae	*Sphyraena barracuda*	DLNR-DAR CML 2004-2013; WPRFMC Hawaii FEP 2009; McCoy et al 2018
	Sphyraena helleri	DLNR-DAR CML 2004-2013; WPRFMC Hawaii FEP 2009; McCoy et al 2018

The Hawai‘i Coral Reef Strategy (HCRS) developed a list of 10 fish species that were deemed as important species for nearshore fisheries for further consideration in assessments and management under the Coral Reef Conservation Program's Fisheries Pillar. Those 10 species are: *Chlorurus perspicillatus* (uhu 'ahu'ula/uliuli), *Chlorurus spilurus* (uhu), *Scarus rubroviolaceus* (uhu pālukaluka/'ele'ele), *Ctenochaetus strigosus* (kole), *Acanthurus triostegus* (manini), *Naso unicornis* (kala), *Kyphosus spp.* (nenue), *Parupeneus porphyreus* (kumu), *Caranx ignobilis* (white ulua), and *Caranx melampygus* (omilu).

To prioritize species for inclusion in our analyses, we considered the data in Table 1, and consulted with Council staff. With these, and given the relevance of this work to fisheries management policy, we focused on the 10 species identified by the HCRS and their associated families and functional groups. Of those, we were not able to include *Caranx ignobilis* (white ulua) because they were observed too rarely to properly estimate a probability of presence. For all analyses we focused on biomass, and also included a metric of total fish biomass to compare the efficacy of species and species groupings for EBFM applications.

Data for indicators were previously compiled from existing underwater visual surveys collected by monitoring programs by the Hawai‘i Monitoring and Reporting Collaborative (Donovan et al. 2018). The database consists of >12,000 surveys of both fish and benthic data from 2000-2020 (Figure 3). We used a subset of this overall dataset, focused on 2004-2014 to align with other analyses being conducted from this dataset, and to best match the driver datasets described below that represent the best available data to meet our objectives.

In total, data from 5,806 surveys were included in the analyses, where a survey is defined as a unique latitude, longitude, year, and depth conducted with a given method. Data were from multiple methods used to survey fish assemblages from five major monitoring programs: the State of Hawai‘i Division of Aquatic Resources, the National Oceanic and Atmospheric Administration National Coral Reef Monitoring Program, the Nature Conservancy Hawai‘i, the University of Hawai‘i, and the National Park Service. Prior to analyses done here, biomass was calculated for each indicator at each survey using existing length-weight conversions, and were calibrated to account for differences in methodologies. Details on how data were treated can be found in Donovan et al. (2018).

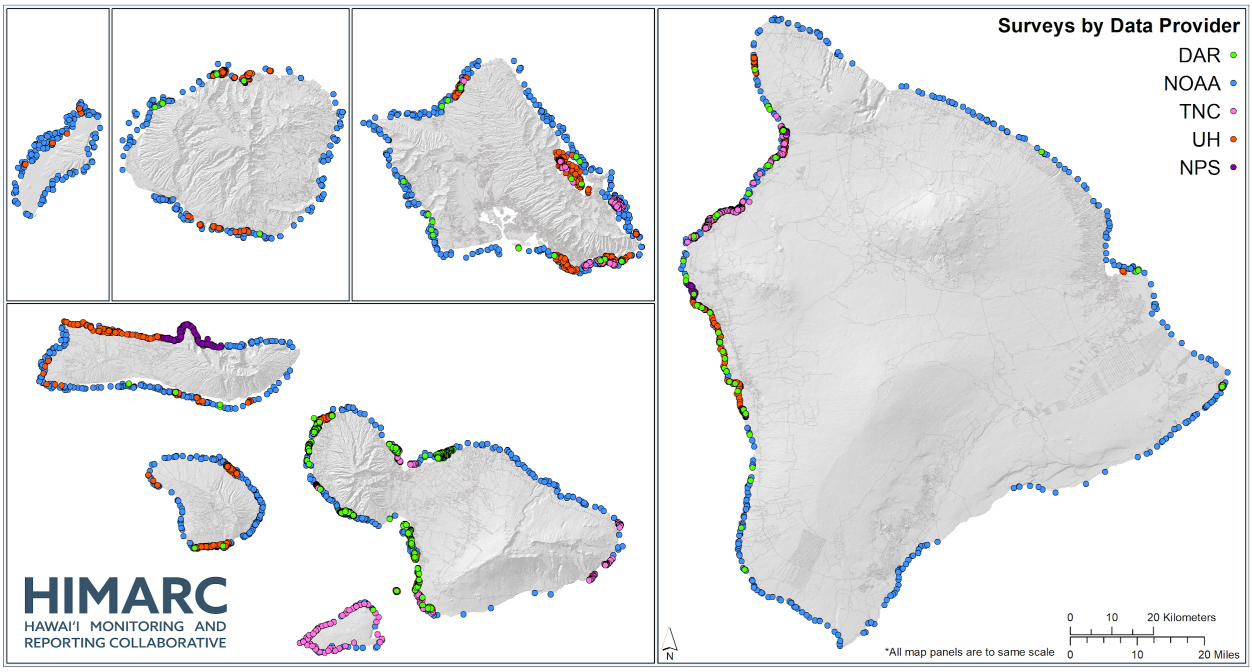

Figure 3. Spatial distribution of sampling from different data providers (colored circles) in the HIMARC database. Data providers are as follows: State of Hawai'i Division of Aquatic Resources (DAR); National Oceanic and Atmospheric Administration (NOAA); The Nature Conservancy (TNC); University of Hawai'i (UH); and the U.S. National Park Service (NPS).

We then paired indicators with drivers with a focus on environmental (physical, oceanographic, and habitat) variables. Due to the importance of first establishing an understanding of the fundamental relationships between the ecological indicators and the natural system, we chose to focus on environmental drivers rather than those associated with humans (e.g., fishing, land-based pollution).

Environmental driver data relied heavily on previous work completed by the Ocean Tipping Points Project (Wedding et al. 2018). Environmental layers were built based on methodological approaches and results presented in Gove et al. (2013) to develop fine-resolution modeled and satellite-based metrics of four environmental drivers for Hawai'i including: sea surface temperature, chlorophyll-a, irradiance, and wave forcing. Predictors were chosen from a set of 4 total variables consisting of multiple metrics for several sets of predictors (e.g., mean, max, standard deviation; Table 2). We also included continuous variables representing depth and rugosity (habitat complexity) that were derived from multiple sources of remotely sensed data since no one source has complete coverage for all nearshore areas (Donovan et al. in prep). We grouped all predictors into 1) physical and oceanographic, and 2) habitat factors. After considering correlations among variables, 10 predictors were selected for inclusion in our models.

Table 2. Environmental drivers and data sources.

Physical and Oceanographic		
Temperature standard deviation	Mean and standard deviation of sea surface temperature from weekly 5 km NOAA blended satellite data from 2000-2013	Wedding et al. 2018
Temperature long-term mean		
Irradiance long-term mean	Mean solar radiation at the ocean surface from 4 km MODIS, 8-day composites from 2002-2013	Wedding et al. 2018
Wave anomaly maximum	Wave power anomaly maximum and frequency from 0.5-1 km hourly data from the Simulating Waves Nearshore (SWAN) model from 2000-2013	Wedding et al. 2018
Wave anomaly frequency		
Chl-*a* anomaly maximum	Chlorophyll-*a* long-term mean, and anomaly frequency and maximum from 4 km MODIS, 8-day composites from 2002-2013	Wedding et al. 2018
Chl-*a* anomaly frequency		
Chl-*a* long-term mean		
Habitat		
Depth	Blended depth from in situ surveys, 1999-2001 LiDAR surveys conducted by the Army Corps of Engineers (SHOALS), LiDAR surveys conducted by the Army Corps of Engineers in 2013 (CZMIL), and imaging spectroscopy data provided by Arizona State University's Global Airborne Observatory (Asner et al. 2020).	Donovan et al. in prep
Complexity (Rugosity)	Blended slope of slope from 1999-2001 LiDAR surveys conducted by the Army Corps of Engineers (SHOALS), LiDAR surveys conducted by the Army Corps of Engineers in 2013 (CZMIL), and imaging spectroscopy data provided by Arizona State University's Global Airborne Observatory (Asner et al. 2020).	Donovan et al. in prep

While we were able to explore the option of updating the environmental driver layers (see interim reports), we made the decision to base our analyses 2004-2014 to align with previously conducted analyses, and to align with data compiled for the Ocean Tipping Points project that was for a period representative of the data at the time of that project (2000-2013).

Screening for nonlinear relationships

To screen for nonlinearities in our indicator and ecosystem driver relationships, we used several quantitative tools to better understand thresholds in the indicator-driver pairs. The use of multi-model inference by incorporating multiple statistical methods to define the relationship between an ecosystem indicator and driver offers a quantitative basis for ecosystem management, with thresholds lending utility for defining effective management targets and assessing management actions after implementation. Following a protocol developed for EBFM in the California Current (Samhouri et al. 2017), we screened for potential nonlinearities in the spatial relationships between the selected ecosystem indicators (species, species complexes, and functional groups) and environmental drivers.

Gradient forest analyses

Gradient forest analyses were used to first screen potential indicator-driver relationships for nonlinearities (Large et al. 2015, Tam et al. 2017, Samhouri et al. 2017). Gradient forests are sets of regression trees that can be applied to a set of relationships to identify splits in the data that maximize homogeneity (Ellis et al. 2012). The advantage of this method is that it considers multiple indicators together along a gradient of a pressure variable. Thus, if more than one indicator responds to a pressure at a similar level there is a good chance of revealing cumulative effects. Gradient forest analysis was implemented with the *gradientForest* package in the R Language for Statistical Computing.

To screen the suite of identified indicators for inclusion in the gradient forest analysis, a random forest model was fit for each individual indicator with the environmental drivers. If an indicator had no variance explained by random forests ($R^2 = 0$), they were not included in the gradient forest model. After screening indicators with random forest models, a gradient forest model was fit for all significant indicators (from the random forest analysis) with the full suite of environmental drivers as predictors. The importance of each driver was then calculated based on maximizing the homogeneity of variance of the indicator values for each partition. Environmental drivers that had an $R^2 \geq 0.01$ were considered further to assess potential threshold relationships.

Generalized Additive Mixed Models

To examine each indicator-driver relationship in more detail, we used Generalized Additive Mixed Models (GAMMs; *mgcv* package in R). For each GAMM, we used a thin plate regression smoothing spline for the environmental driver fixed effect, with a basis dimension set to 4 to reduce model overfitting (Large et al. 2013). The random effects of 'island', 'dataset', and 'habitat type' were also included in each model to account for variation in these factors across our indicator data. Because of the prominence of zero-inflation in the fish biomass data, two separate GAMMs were fit for each of the driver (n = 10) and indicator (n = 19) pairs (380 models in total). The first model was based on indicator presence or absence, using a binomial distribution with a logit link (Equation 1). The second model was for presence-only indicator biomass, and modeled with a gamma distribution and a log link (Equation 2).

For both models, we defined E_i as the value of the ecological indicator at survey i, with α as a fixed intercept, D_i as the value of the driver for survey i, s( ) the thin plate regression spline smoothing function, γ, δ, and ω as the categorical variables 'island', 'dataset', and 'habitat type', respectively, and ε as a normally distributed random error term.

$$logit(E_{ijkl}) = \alpha + s(D_i) + \gamma_j + \delta_k + \omega_l + \varepsilon_i \qquad [1]$$

$$ln(E_{ijkl}) = \alpha + s(D_i) + \gamma_j + \delta_k + \omega_l + \varepsilon_i \qquad [2]$$

A significant threshold response for each GAMM was defined by three criteria: (1) model estimated degrees of freedom (edf) > 2 (Zuur et al. 2013, Hunsicker et al. 2016); (2) driver (fixed effect) p-value ≤ 0.05; and (3) model deviance explained ≥ 0.20.

Screening nonlinearities results

The initial screening of 19 indicators with the random forest for subsequent inclusion in the gradient forest included indicator mean prediction performance (R^2) between 0 and 0.46 (Table 3). Notably, there were four indicators with an $R^2 = 0$: *Acanthurus triostegus* (manini), *Parupeneus porphyreus* (kumu), *Chlorurus perspicillatus* (uhu 'ahu'ula/uliuli), and the functional group grazers. As such, these indicators were not included in the gradient forest model.

Table 3. Random forest screening output for individual indicators. Indicators in gray indicate random forests with an $R^2 = 0$, and were not included in the subsequent gradient forest analysis.

Indicator	Random forest R^2
Total biomass	0.184
Scrapers / Excavators	0.083
Scaridae	0.092
Chlorurus spilurus	0.215
Chlorurus perspicillatus	0.000
Scarus rubroviolaceus	0.023
Grazers	0.000
Acanthuridae	0.045
Ctenochaetus strigosus	0.457
Acanthurus triostegus	0.000
Naso unicornis	0.082
Kyphosidae	0.004
Browsers	0.110
Secondary consumers	0.103
Mullidae	0.011
Parupeneus porphyreus	0.000
Piscivores	0.070
Carangidae	0.003
Caranx melampygus	0.012

The gradient forest model, with 15 indicators and the full suite of 10 environmental drivers, highlighted four drivers that surpassed the R^2 importance threshold of 0.01, indicating that these four drivers (rugosity, wave anomaly maximum, depth, and wave anomaly frequency) all had significant thresholds with one or more indicators (Figure 4).

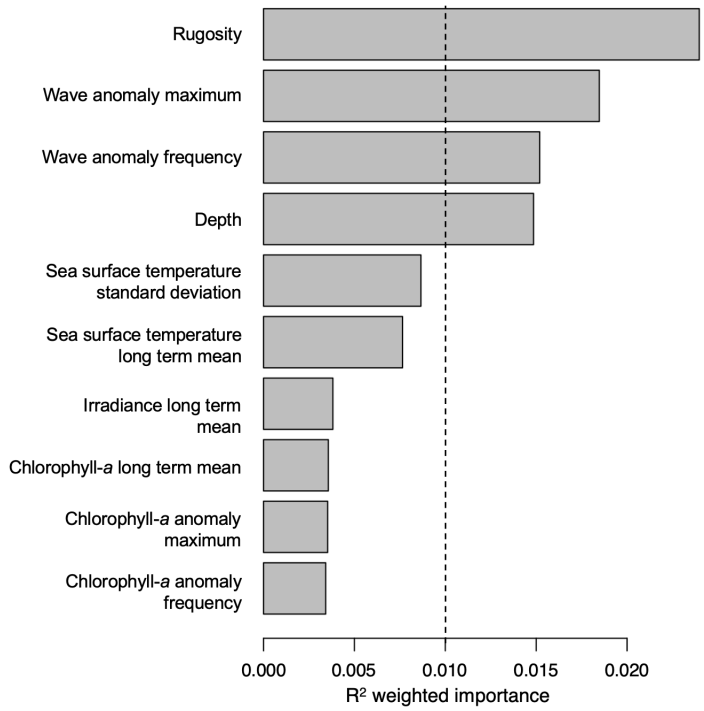

Figure 4. Weighted importance (R^2) of each environmental driver in the gradient forest analysis across ecological indicator outputs. The dashed line represents the $R^2 = 0.01$ threshold for identification of significant threshold relationships.

However, indicator-specific responses to the four identified environmental drivers varied widely. Using the unitless cumulative predictive performance (R^2) of each indicator, we can directly compare the magnitudes of indicator responses within and across drivers. *Ctenochaetus strigosus* (kole) biomass had high cumulative importance for all four environmental drivers, but exhibited more gradual shifts along the driver gradient (Table 4; Figure 5).

Table 4. Mean predictive performance (R^2) of the gradient forest analysis for each indicator-driver pair included in the best model (environmental drivers that met the overall $R^2 = 0.01$ threshold significance).

Indicator	**Wave anomaly frequency**	**Wave anomaly maximum**	**Depth**	**Rugosity**
Total biomass	0.033	0.047	0.022	0.038
Scrapers / Excavators	0.013	0.014	0.013	0.017
Scaridae	0.014	0.016	0.015	0.019
Chlorurus spilurus	0.028	0.040	0.026	0.058
Scarus rubroviolaceus	0.005	0.006	0.001	0.002
Acanthuridae	0.012	0.008	0.004	0.009
Ctenochaetus strigosus	0.066	0.078	0.077	0.072
Naso unicornis	0.005	0.004	0.008	0.064
Kyphosidae	0.001	0.003	0.001	0.001
Browsers	0.005	0.006	0.019	0.061
Secondary consumers	0.017	0.019	0.008	0.010
Mullidae	0.001	0.002	0.000	0.001
Piscivores	0.016	0.017	0.014	0.006
Carangidae	0.007	0.011	0.003	0.001
Caranx melampygus	0.004	0.004	0.010	0.001

In contrast, both *Naso unicornis* (kala) and the functional group browsers had a strong threshold with rugosity at values between 20-25 of the rugosity index (Table 4; Figure 5d). Total fish

biomass and *Chlorurus spilurus* (uhu) also had relatively high cumulative importance associated with rugosity, wave anomaly maximum, and wave anomaly frequency (Table 4; Figures 5a,b,d), while all other included indicators had responses with lower cumulative importance, but with significant thresholds nonetheless (Table 4). Interestingly, the cumulative predictive performance curves for Scaridae, *Chlorurus spilurus* (uhu), and functional group scrapers/excavators are very similar to each other for each of the environmental drivers, which is expected as Scaridae and *Chlorurus spilurus* are within the scraper/excavator functional group. A similar paired response is also observed for *Naso unicornis* kala and browsers with the environmental driver rugosity (Figure 5d).

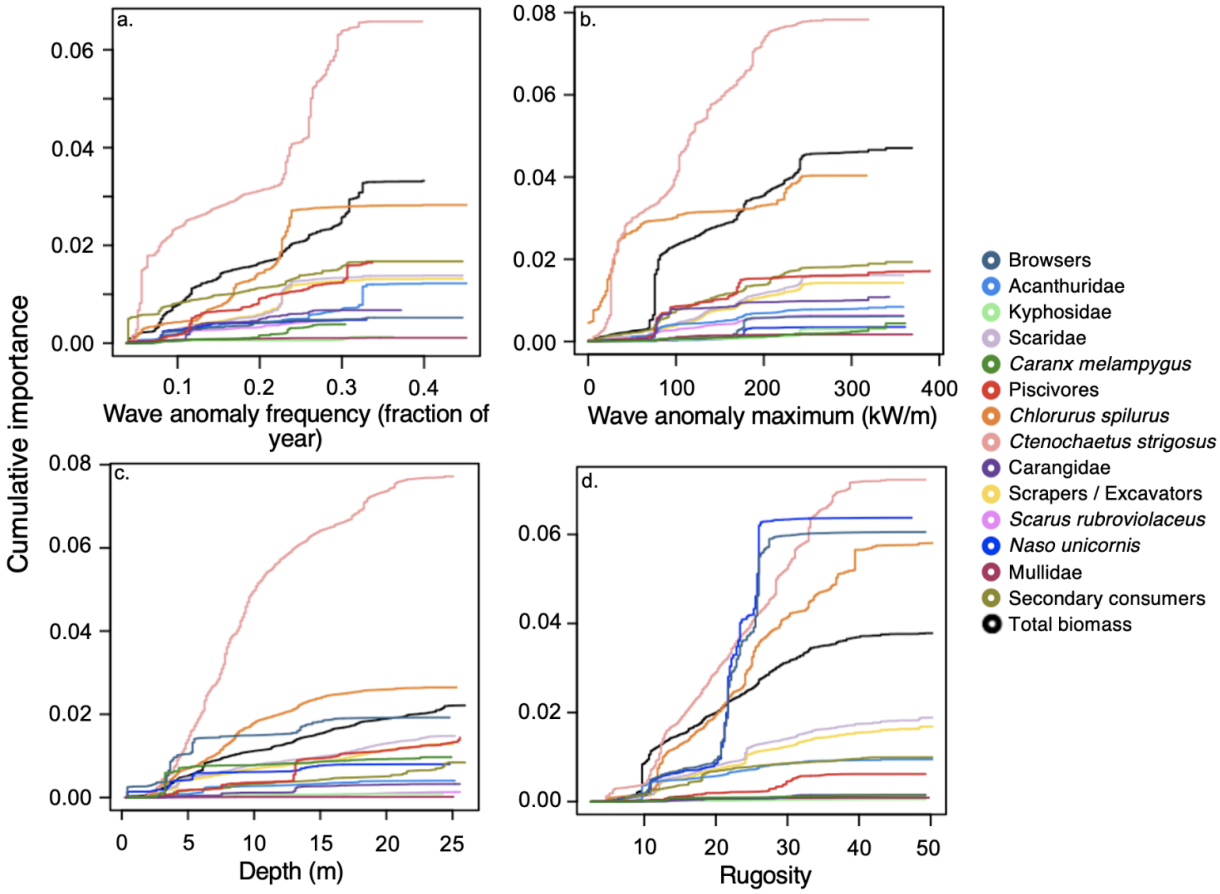

Figure 5. Cumulative importance (R^2) of each indicator (colored lines) for a given environmental driver (panels) in the gradient forest analysis: (a) wave anomaly frequency (fraction of year), (b) wave anomaly maximum (kW/m), (c) depth (m), and (d) rugosity.

GAMMs revealed several strong nonlinear relationships in indicator-driver pairs, with 42 models meeting the significance criteria across the binomial- and gamma-distributed GAMMs. Eleven indicators had at least one significant nonlinear relationship with an environmental driver, while all environmental drivers had a significant nonlinearity identified with at least one indicator. Model deviance explained ranged from 0.20 to 0.38.

Of the 190 binomial GAMMs (indicator presence-absence), 26 models had significant nonlinearities across six indicators (Figure 6). *Chlorurus spilurus* (uhu) had strong nonlinear

relationships with six environmental drivers, chlorophyll-*a* anomaly frequency and long term mean, irradiance long term mean, sea surface temperature long term mean, rugosity, and depth (GAMM deviance explained ranging from 0.22-0.25, p = 0-0.027). The functional group grazers had strong nonlinear relationships with six environmental drivers as well, chlorophyll-*a* anomaly frequency and maximum, wave anomaly frequency, sea surface temperature long term mean, rugosity, and depth (deviance explained = 0.20-0.22, p = 0-0.023). Family Acanthuridae had eight nonlinear relationships, including chlorophyll-*a* anomaly frequency and maximum, wave anomaly frequency and maximum, irradiance long term mean, sea surface temperature standard deviation, rugosity, and depth (deviance explained = 0.22-0.29, p = < 0.01). *Ctenochaetus strigosus* (kole) had two nonlinearities identified, including rugosity and depth (deviance explained = 0.25, p < 0.01). Kyphosidae had three nonlinearities, including wave anomaly maximum, irradiance long term mean, and rugosity (deviance explained = 0.21-0.22, p < 0.01), and the functional group secondary consumers had a strong nonlinearity identified with chlorophyll-*a* anomaly frequency (deviance explained = 0.38, p = 0.003).

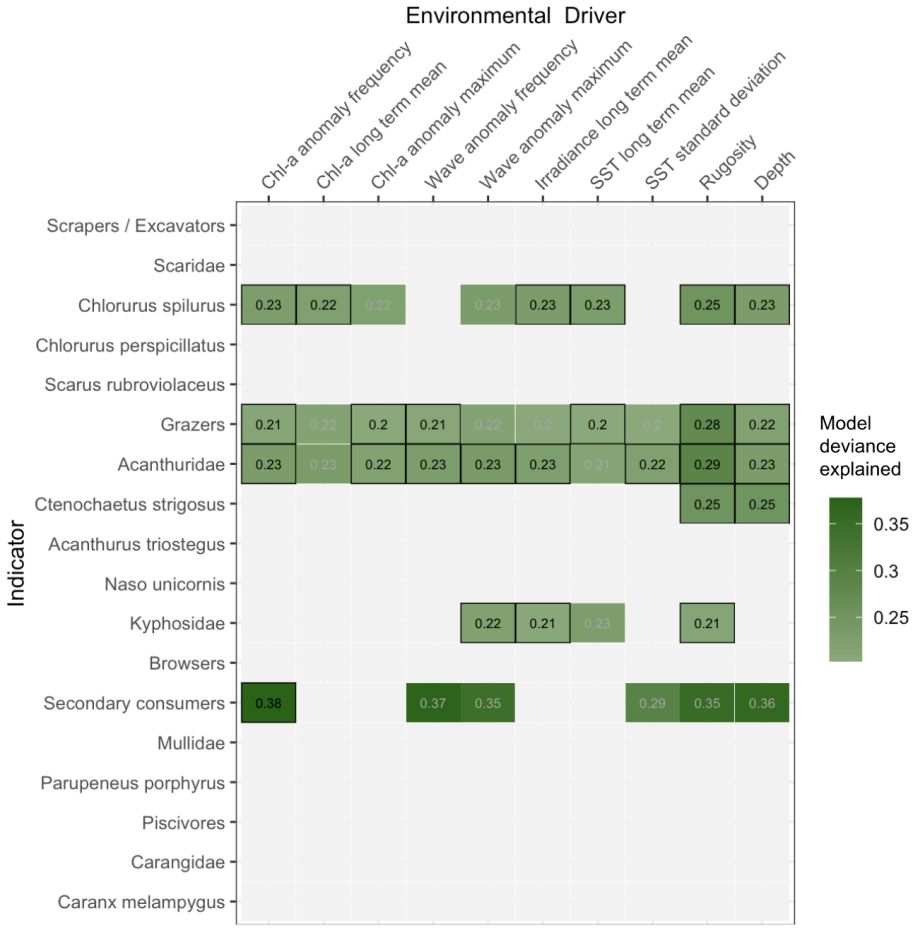

Figure 6. Model summaries for binomially distributed GAMMs fit with indicator presence-absence data. The color gradient and cell values reflect the model deviance explained for the indicator-driver pairs. Cells with a black bounding box show indicator-driver pairs with significant nonlinear relationships that meet all criteria. Cells with color but no bounding box did not meet our model deviance explained significance threshold. A gray cell indicates no significant nonlinear relationship between the given indicator and driver.

The 190 GAMMs with a gamma-distributed response (indicator presence-only biomass) had fewer significant nonlinear relationships with the environmental indicators, with 16 strong nonlinearities identified across six indicators (Figure 7). *Chlorurus perspicillatus* (uhu 'ahu'ula/uliuli) had one nonlinearity identified with irradiance long term mean (GAMM deviance

explained = 0.25, p = 0.047), while *Naso unicornis* (kala) had five significant nonlinear relationships identified: chlorophyll-a long term mean and anomaly maximum, wave anomaly frequency, sea surface temperature long term mean and standard deviation (deviance explained = 0.25-0.27, p = 0-0.03). The family Kyphosidae had four significant nonlinearities: wave anomaly frequency and maximum, irradiance long term mean, and sea surface temperature long term mean (deviance explained = 0.28-0.29, p = 0.001-0.035). The functional group browsers also had four strong nonlinearities: chlorophyll-*a* long anomaly frequency and long term mean, sea surface temperature long term mean, and depth (deviance explained = 0.21-0.23, p < 0.01). The functional group piscivores had one significant nonlinearity with sea surface temperature long term mean (deviance explained = 0.21, p < 0.01), while Carangidae had one nonlinearity identified with chlorophyll-*a* anomaly frequency (deviance explained = 0.23, p = 0.022).

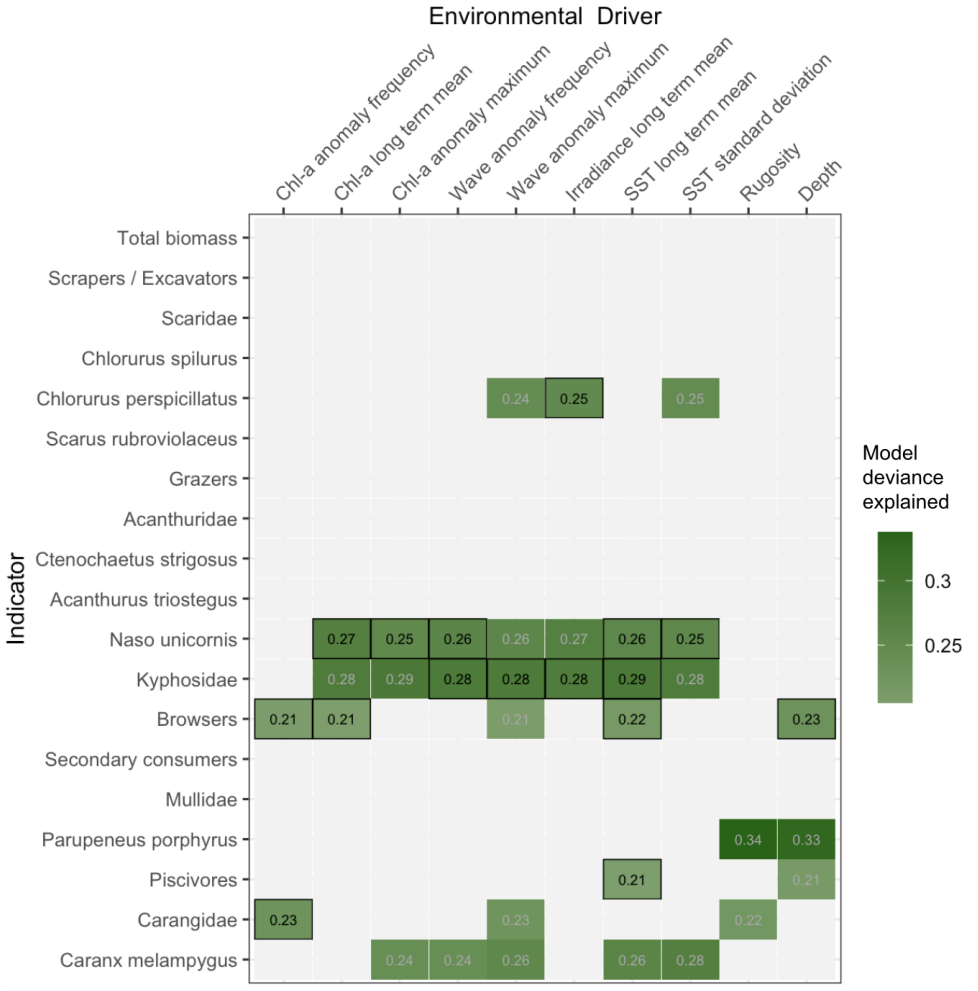

Figure 7. Model summaries for binomially distributed GAMMs fit with indicator presence-only data. The color gradient and cell values reflect the model deviance explained for the indicator-driver pairs. Cells with a black bounding box show indicator-driver pairs with significant nonlinear relationships that meet all criteria. Cells with color but no bounding box did not meet our model deviance explained significance threshold. A gray cell indicates no significant nonlinear relationship between the given indicator and driver.

Multi-model inference: comparing identified nonlinearities across model frameworks

Using the fitted gradient forest and GAMM analyses, we compared indicator and pressure relationships identified as nonlinear in both analyses to better understand these relationships across multiple lines of evidence. Of the 190 distinct indicator-driver pairs, 83 had significant

nonlinearities identified by the GAMM or gradient forest analysis. Notably, neither *Parupeneus porphyreus* (kumu) nor *Acanthurus triostegus* (manini) had significant nonlinearities identified with any driver across all models, while the family Kyphosidae was the only indicator with a nonlinearity with an environmental driver identified by all three types of models (gradient forest, binomial GAMM, gamma GAMM).

Of the 83 significant nonlinearities identified, 13 were supported by both the gradient forest analysis as well as at least one type of GAMM (binomially-distributed, gamma-distributed, or both). These significant nonlinear relationships supported by multi-model inference included 6 indicators: the families Acanthuridae and Kyphosidae, the functional group browsers, and the species *Ctenochaetus strigosus* (kole), *Naso unicornis* (kala), and *Chlorurus spilurus* (uhu), as well as 4 environmental drivers: rugosity, wave anomaly maximum, wave anomaly frequency, and depth (Table 5).

Table 5. Summary of significant nonlinear relationships identified across indicator-driver pairs. Indicators and drivers in **bold** indicate a significant nonlinear relationship that was supported by multiple modeling frameworks (*i.e.,* at least one GAMM model as well as the Gradient Forest analysis).

Indicator	Driver/Pressure	Analysis
Total biomass	Wave anomaly frequency	Gradient Forest
	Wave anomaly maximum	Gradient Forest
	Rugosity	Gradient Forest
	Depth	Gradient Forest
Scrapers / Excavators	Wave anomaly frequency	Gradient Forest
	Wave anomaly maximum	Gradient Forest
	Rugosity	Gradient Forest
	Depth	Gradient Forest
Scaridae	Wave anomaly frequency	Gradient Forest
	Wave anomaly maximum	Gradient Forest
	Rugosity	Gradient Forest
	Depth	Gradient Forest
Chlorurus spilurus	Chl-a anomaly frequency	Binomial GAMM
	Chl-a anomaly long term mean	Binomial GAMM
	Wave anomaly frequency	Gradient Forest
	Wave anomaly maximum	Gradient Forest
	Irradiance long term mean	Binomial GAMM
	SST long term mean	Binomial GAMM
	Rugosity	**Binomial GAMM; Gradient Forest**
	Depth	**Binomial GAMM; Gradient Forest**
Chlorurus perspicillatus	Irradiance long term mean	Gamma GAMM
Scarus rubroviolaceus	Wave anomaly frequency	Gradient Forest
	Wave anomaly maximum	Gradient Forest
	Rugosity	Gradient Forest
	Depth	Gradient Forest
Grazers	Chl-a anomaly frequency	Binomial GAMM
	Chl-a anomaly maximum	Binomial GAMM
	Wave anomaly frequency	Binomial GAMM
	SST long term mean	Binomial GAMM
	Rugosity	Binomial GAMM
	Depth	Binomial GAMM

Acanthuridae	Chl-a anomaly frequency	Binomial GAMM
	Chl-a anomaly maximum	Binomial GAMM
	Wave anomaly frequency	**Binomial GAMM; Gradient Forest**
	Wave anomaly maximum	**Binomial GAMM; Gradient Forest**
	Irradiance long term mean	Binomial GAMM
	SST standard deviation	Binomial GAMM
	Rugosity	**Binomial GAMM; Gradient Forest**
	Depth	**Binomial GAMM; Gradient Forest**
Ctenochaetus strigosus	Wave anomaly frequency	Gradient Forest
	Wave anomaly maximum	Gradient Forest
	Rugosity	**Binomial GAMM; Gradient Forest**
	Depth	**Binomial GAMM; Gradient Forest**
Naso unicornis	Chl-a long term mean	Gamma GAMM
	Chl-a anomaly maximum	Gamma GAMM
	Wave anomaly frequency	**Gamma GAMM; Gradient Forest**
	Wave anomaly maximum	Gradient Forest
	SST long term mean	Gamma GAMM
	SST standard deviation	Gamma GAMM
	Rugosity	Gradient Forest
	Depth	Gradient Forest
Kyphosidae	**Wave anomaly frequency**	**Gamma GAMM; Gradient Forest**
	Wave anomaly maximum	**Binomial GAMM; Gamma GAMM; Gradient Forest**
	Irradiance long term mean	Binomial GAMM; Gamma GAMM
	SST long term mean	Gamma GAMM
	Rugosity	**Binomial GAMM; Gradient Forest**
	Depth	Gradient Forest
Browsers	Chl-a anomaly frequency	Gamma GAMM
	Chl-a long term mean	Gamma GAMM
	Wave anomaly frequency	Gradient Forest
	Wave anomaly maximum	Gradient Forest
	SST long term mean	Gamma GAMM
	Rugosity	Gradient Forest
	Depth	**Gamma GAMM; Gradient Forest**
Secondary consumers	Chl-a anomaly frequency	Binomial GAMM
	Wave anomaly frequency	Gradient Forest
	Wave anomaly maximum	Gradient Forest
	Rugosity	Gradient Forest
	Depth	Gradient Forest
Mullidae	Wave anomaly frequency	Gradient Forest
	Wave anomaly maximum	Gradient Forest
Piscivores	Wave anomaly frequency	Gradient Forest
	Wave anomaly maximum	Gradient Forest
	SST long term mean	Gamma GAMM
	Rugosity	Gradient Forest
	Depth	Gradient Forest
Carangidae	Chl-a anomaly frequency	Gamma GAMM
	Wave anomaly frequency	Gradient Forest
	Wave anomaly maximum	Gradient Forest
	Rugosity	Gradient Forest
	Depth	Gradient Forest
Caranx melampygus	Wave anomaly frequency	Gradient Forest
	Wave anomaly maximum	Gradient Forest

What is the shape of nonlinear relationships, and how strong are the thresholds?

Threshold identification methods

With each indicator-driver pair screened for nonlinearities, 13 significant nonlinear relationships were supported by multi-model inference to examine in more detail. Using the fitted GAMMs, we calculated the first and second derivatives of the fitted relationships to identify the location of potential thresholds in these nonlinear relationships (following (Large et al. 2013)). To do this, we first bootstrapped each GAMM fit (sample n = 3000, n bootstrap = 1000), and used the bootstrapped fits to construct a 95% confidence interval of the GAMM driver smoothing function. We then took the second derivative of the smoother across each bootstrap to identify threshold locations. We defined thresholds as the driver ranges over which 95% interval of the GAMM second derivative did not overlap zero, with our best estimate of each threshold point estimate as the value of the driver at which the second derivative was most different from zero along the threshold range.

Bayesian hierarchical models

To further confirm the location and confidence around the threshold location, we explored Bayesian hierarchical models that are designed to account for hierarchical spatial scales as well as hierarchy inherent in data synthesized from multiple sources. There are several advantages to using this approach especially in a case such as this where the analysis is based on unbalanced data with several levels of inference (Gelman et al. 2013). However, due to the relative complexity of these methods compared to the flexibility of gradient forests and GAMMs, we were unable to successfully fit these models. Nonetheless, the approach is described here, and is an avenue for further research.

The statistical distribution and link function for each model was chosen specific to each indicator-driver pair to mirror the analyses conducted with the GAMMs. For example, if there was a significant threshold identified with a given indicator-driver pair with a binomially-distributed GAMM, this same pair was modeled with a binomial distribution and logit link. We explored implementation of the models with the *R* statistical environment with extensions to the two software programs: JAGS (Just Another Gibbs Sampler) (Plummer 2016) and Stan (Carpenter et al. 2017).

To evaluate the existence of threshold values between indicator species and environmental drivers, we constructed five candidate models: null (intercept-only), linear, step-wise, piecewise, and general models following (Qian and Cuffney 2012), with the following forms:

The null model: $$y = \beta_0 + \varepsilon \quad [1]$$

The linear model: $$y = \beta_0 + \beta_1 x + \varepsilon \quad [2]$$

The step-wise model: $$y = [\beta_0 + \varepsilon_1 \; if \; x < \phi \quad \beta_0 + \delta + \varepsilon_2 \; if \; x \geq \phi \quad [3]$$

The piecewise model: $$y = [\beta_0 + \delta x + \varepsilon_1 \; if \; x < \phi \quad \beta_0 + \delta x + \alpha * (x - \phi) + \varepsilon_2 \; if \; x \geq \phi \quad [4]$$

The general model: $$y = [\beta_0 + \beta_1 x + \varepsilon_1 \; if \; x < \phi \quad (\beta_0 + \delta_0) + (\beta_1 + \delta_1) x + \varepsilon_2 \; if \; x \geq \phi \quad [5]$$

where *y* is the ecosystem indicator, *x* is the driver, and ϕ is the threshold value. The existence of the threshold can be identified by fitting all five models and using model selection to compare against the null and linear models. Further model diagnostics from visual inspections of residual values are also recommended by (Qian 2014).

Our lack of success in fitting these models is due to a number of factors. The models proposed by (Qian and Cuffney 2012) were designed for indicators that follow a normal distribution, and did not include hierarchical effects. Extending Qian's methods along both of these lines adds several levels of complexity, so a more extensive effort is required to fully understand the implications of these extensions and to properly explore the parametrizations necessary to uncover the thresholds.

Threshold Results

Wave anomaly frequency

Three indicators had significant nonlinearities identified with wave anomaly frequency, all supported by gradient forest model and either binomial (presence-absence) or gamma (presence-only) GAMMs (Figure 8; Table 5): Acanthuridae, *Naso unicornis* (kala), and Kyphosidae.

Acanthuridae presence was generally high for all values of wave anomaly frequency, except for a slight decline in presence between wave anomaly frequency values of 0.1-0.2 (GAMM deviance explained = 0.23, $p < 0.01$; Figure 8a). Three thresholds were identified in this relationship, one ranging from 0.04 to 0.12, with a best estimate of 0.08, one ranging from wave anomaly frequency values of 0.19 to 0.21, with a point estimate of 0.2, and the third ranging from 0.33 to 0.41, with an estimated threshold at 0.33 (Table 6). The third threshold was also supported by the gradient forest analysis, with the estimated range overlapping the GAMM threshold point estimate (Figure 12a).

Naso unicornis (kala) exhibited increases in biomass where present to a local maximum in areas where wave anomaly frequency is about 0.1 (anomalies occurring 10% of the year), and is also predicted to increase with wave anomaly frequencies of above 0.25 (deviance explained = 0.26, $p = 0.007$; Figure 8b). There were two thresholds identified with wave anomaly frequency. The first occurred from values of 0.08 to 0.13 with a best estimate at 0.11, or around the predicted peak in wave anomaly frequency, while the other ranged from 0.17 to 0.33 with a threshold estimate of 0.33 (Table 6). The gradient forest analysis provided further support for the first threshold, with the estimated range overlapping the GAMM threshold range and point estimate (Figure 12a).

Additionally, where present, Kyphosidae biomass increased to a local maximum in areas with wave anomaly frequency is about 0.1, and is also predicted to increase with wave anomaly frequencies of above 0.25 (deviance explained = 0.28, $p = 0.01$; Figure 8c). This relationship

also had a threshold from values of 0.24 to 0.33, with the best estimate of the threshold location at the wave anomaly maximum value of 0.33 (Table 6). This threshold was also supported by the gradient forest analysis, with the estimated threshold overlapping with the estimated GAMM threshold range (Figure 12a).

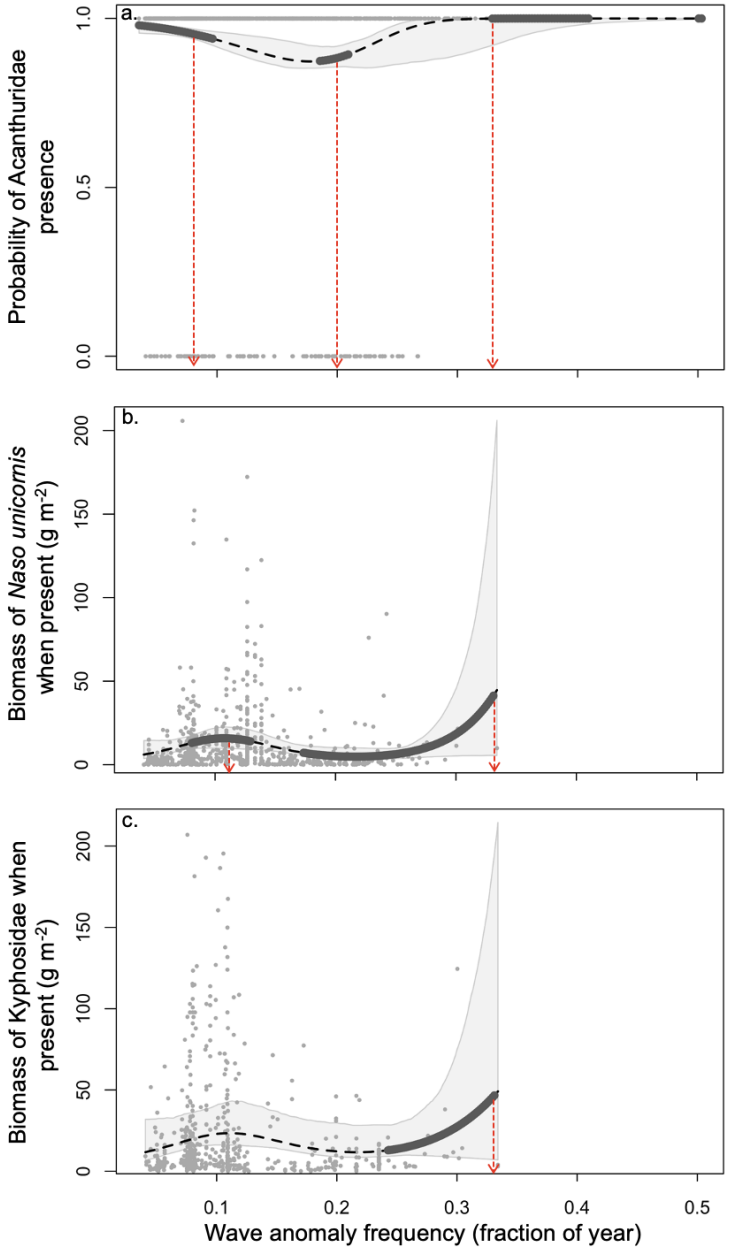

Figure 8. Fitted GAMMs for (a) the probability of family Acanthuridae presence, (b) *Naso unicornis* (kala) presence-only biomass (g m^{-2}), and (c) Kyphosidae presence-only biomass (g m^{-2}) with wave anomaly frequency. The black dashed line is the GAMM smoothed function, the shaded interval represents the bootstrapped 95% confidence interval, and the gray points are the raw data. The bold line indicates the threshold range where the 95% CI of the second derivative does not include 0, while the dashed red lines show the best estimates for threshold locations (i.e., where the second derivative is most different from zero within the threshold range).

There were commonalities and differences in each indicator's nonlinear relationship with wave anomaly frequency in both magnitude of response as well as threshold location. In particular, patterns of the fitted relationships were similar for both browsers, *Naso unicornis* (kala) and Kyphosidae, although *N. unicornis* had a significant threshold at intermediate values of wave anomaly frequency and Kyphosidae did not. However, the gradient forest analysis did identify an additional threshold for Kyphosidae that overlapped with this *N. unicornis* threshold, although

it was not identified in the GAMM analysis. Interestingly, the two indicators were not correlated with each other (Figure S1, Pearson's correlation = 0.02), but had very similar responses to the driver. This pattern is contrary to the family-level threshold identified for Acanthuridae, however, which showed decreased presence at wave anomaly frequency values of 0.1-0.2. While the Acanthuridae model was modeling the probability of presence and kala's significant threshold relationship with wave anomaly frequency was supported with a presence-only biomass (g m^{-2}) response, these contrary results suggest that kala associations with the environmental drivers may not be well described by family-level trends.

Wave anomaly maximum

Two indicators had significant nonlinearities identified with wave anomaly maximum: Acanthuridae and Kyphosidae (Figure 9; Table 5).

A nonlinearity with Acanthuridae was supported by the gradient forest model and a binomial (presence-absence) GAMM. Acanthuridae presence increased with wave anomaly maximum (peak presence = 150 kW/m, deviance explained = 0.23, $p < 0.01$; Figure 9a). One threshold was identified, ranging from 0 to 134.3 kW/m, with the best estimate of the threshold location at 22 kW/m (Table 6). The threshold was also supported by the gradient forest analysis, with the estimated range overlapping the GAMM threshold range (Figure 12b).

Kyphosidae had significant nonlinearities with wave anomaly maximum supported by the gradient forest model as well as both binomial (presence-absence) and gamma (presence-only) GAMMs (binomial GAMM: deviance explained = 0.22, $p < 0.01$; gamma GAMM: deviance explained = 0.28, $p = 0.004$). While the two different GAMM response structures are distinct, the general form of the relationship with wave anomaly maximum was consistent across models. Both GAMMs revealed a local peak in Kyphosidae probability of presence or presence-only biomass (g m^{-2}) at values around 100, with a decline and subsequent increase at higher values of wave anomaly maximum (Figures 9b,c). This relationship was more strongly nonlinear when modeled as presence-absence rather than presence-only biomass (edf = 3 and 2.5, respectively), but the congruence of modeled relationships across response structure reinforces the significance of Kyphosidae's relationship with wave anomaly maximum. However, thresholds were only identified with the probability of Kyphosidae presence and wave anomaly maximum. The first threshold ranged from 0 to 44.1 kW/m, with the best estimate of the threshold location at 18 kW/m. The second thresholds ranged from 60.1 to 154.4 kW/m with a point estimate of 94.3 kW/m, and the third spanned 190.5 to 312.7 kW/m with a best threshold estimate at 242.6 kW/m (Table 6). The gradient forest analysis provides further support for the third threshold, with the estimated range overlapping the GAMM threshold point estimate (Figure 12b).

The nonlinear relationships of Acanthuridae and Kyphosidae with wave anomaly maximum were similar for the first threshold location, potentially indicating a minimum amount of wave forcing structuring both species groups. There was also a similar general increase in probability of presence (and biomass) up until ~100 kW/m across all three indicators, with the probability of Kyphosidae presence generally increasing throughout the range of wave anomaly frequency. The similarities and differences across the two species groups may indicate some larger

structuring variables at play, especially given that the two groups occupy different functional roles, and Acanthuridae and Kyphosidae are not correlated (Figure S1, Pearson's correlation = 0.06), so the results are in contrast to an expectation that they might have distinct relationships with the driver.

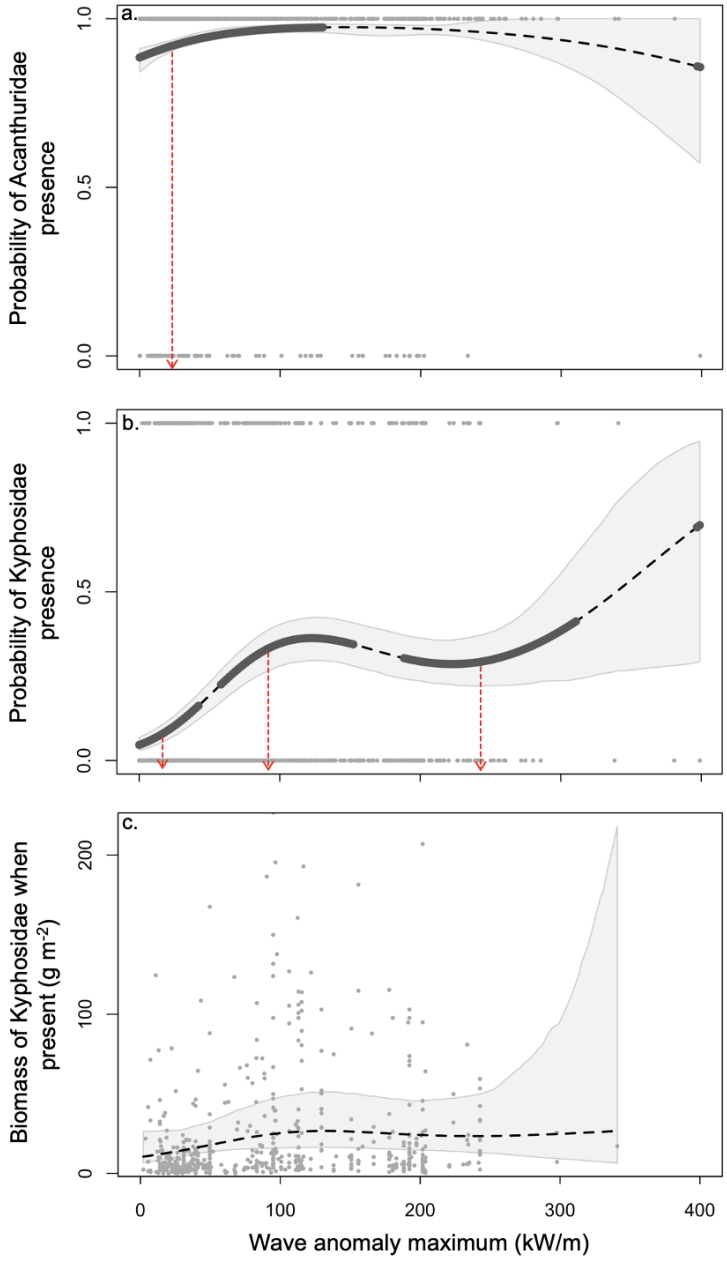

Figure 9. Fitted GAMMs for (a) the probability of family Acanthuridae presence, (b) the probability of family Kyphosidae presence, and (c) Kyphosidae presence-only biomass (g m^{-2}) with wave anomaly maximum. The black dashed line is the GAMM smoothed function, the shaded interval represents the bootstrapped 95% confidence interval, and the gray points are the raw data. The bold line indicates the threshold range where the 95% CI of the second derivative does not include 0, while the dashed red lines show the best estimates for threshold locations (i.e., where the second derivative is most different from zero within the threshold range).

Depth

Four indicators had significant nonlinearities identified with depth (Figure 10; Table 5). Nonlinearities with Acanthuridae, *Ctenochaetus strigosus* (kole), and *Chlorurus spilurus* (uhu) were supported by the gradient forest model and binomial (presence-absence) GAMMs, while a

nonlinear relationship with the functional group browsers was supported by the gradient forest model and a gamma (presence-only) GAMM.

There was a predicted peak in Acanthuridae presence at depths of approximately 7-10 m (deviance explained = 0.23, $p < 0.01$; Figure 10a), with an identified threshold range from 0.2 to 12 m, and the best estimate at 2.8 m (Table 6). This threshold was further supported by the gradient forest analysis, with the estimated threshold encompassing the GAMM threshold point estimate (Figure 12c).

Ctenochaetus strigosus (kole) exhibited a peak in presence at depths of about 10 m (deviance explained = 0.25, $p < 0.01$; Figure 10b). There were three thresholds identified with depth. The first spanned 0.2 to 3.3 m with a threshold estimate of 0.8 m, the second ranged from 3.9 to 13.6 m with the best estimate at 6.4 m, and the third threshold was identified from 18.5 to 25.3 m, with the point estimate at 18.5 m (Table 6). The gradient forest analysis supported all three identified thresholds. For the initial two GAMM thresholds, the estimated gradient forest threshold overlapped the upper portion of the first GAMM threshold range, and encompassed the full threshold range of the second GAMM threshold. There was an additional gradient forest threshold identified that overlapped the third GAMM threshold point estimate (Figure 12c).

Browser presence-only biomass (g m^{-2}) was highest at shallow depths, and decreased with depth (deviance explained = 0.23, $p < 0.01$; Figure 10c). There were two thresholds identified in the predicted relationship. The first ranged from 0.3 to 11.2 m, with the best estimate of the threshold location at 0.5 m. The other threshold spanned 21.1 to 25.4 m and had a point threshold estimate at 23.5 m (Table 6). The first threshold was partially supported by the gradient forest analysis, with the estimated threshold overlapping the middle of the first GAMM threshold range (Figure 12c).

Chlorurus spilurus (uhu) exhibited a peak probability of presence at depths of around 10 m, with a subsequent decline through the remainder of the driver range (deviance explained = 0.23, $p < 0.01$; Figure 10d). There were three thresholds identified with depth. The first threshold occurred at the beginning of the depth range, from 0.29 to 2.5 m, with a threshold estimate of 0.29 m. The second threshold ranged from 3.9 to 14.2 m, with a point estimate of 10.3 m, and the third threshold ranged from 23.2 to 25.9 m with the best estimate of the threshold location at 24.5 m (Table 6). The gradient forest analysis supported the second threshold, with its predicted range encompassing the full range of the GAMM estimated threshold, and also overlapped the part of the upper range of the first GAMM threshold (Figure 12c).

Acanthuridae, *Ctenochaetus strigosus* (kole), *Chlorurus spilurus* (uhu), and browsers all had similar threshold locations at shallow depths (range < 10m, point est. < 5m), although the patterns were not in the same directions. Acanthuridae, *Ctenochaetus strigosus* (kole), and *Chlorurus spilurus* (uhu) increased in probability of presence at shallow depths, while browser biomass when present (g m^{-2}) decreased along the same range. None of the four pairwise relationships exhibit strong correlations (Figures S1-S4).

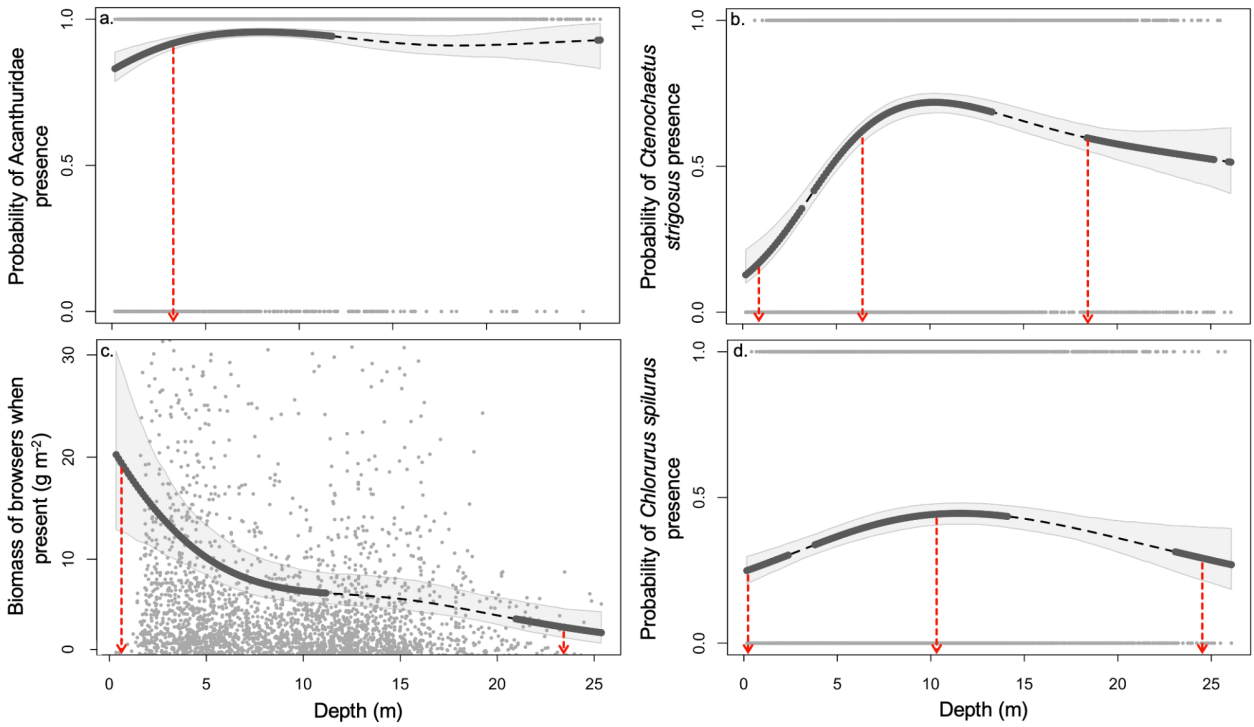

Figure 10. Fitted GAMMs for (a) the probability of family Acanthuridae presence, (b) the probability of *Ctenochaetus strigosus* (kole) presence, (c) functional group browsers presence-only biomass (g m^{-2}) and (d) the probability of *Chlorurus spilurus* (uhu) presence with depth. The black dashed line is the GAMM smoothed function, the shaded interval represents the bootstrapped 95% confidence interval, and the gray points are the raw data. The bold line indicates the threshold range where the 95% CI of the second derivative does not include 0, while the dashed red lines show the best estimates for threshold locations (i.e., where the second derivative is most different from zero within the threshold range).

Rugosity

Four indicators had significant nonlinear relationships identified with rugosity, all supported by gradient forest models and binomial (presence-absence) GAMMs (Figure 11; Table 5): Acanthuridae, *Ctenochaetus strigosus* (kole), Kyphosidae, and *Chlorurus spilurus* (uhu).

Acanthuridae presence increased with increasing rugosity until a peak around 25 (deviance explained = 0.29, $p < 0.01$; Figure 11a) and an identified threshold range from 2.3 to 50.2, with the best estimate at 8.5 (Table 6). The estimated threshold was also supported by the gradient forest analysis, with the estimated range very near the GAMM threshold point estimate, and well within the GAMM threshold range (Figure 12d).

Ctenochaetus strigosus (kole) presence exhibited a marked increase with rugosity to values of approximately 20, with more gradual subsequent decline (deviance explained = 0.25, $p < 0.01$; Figure 11b). There were two thresholds with rugosity identified, with one ranging from 2.3 to 8.8 with a point estimate of 4, and the other ranging from 10.5 to 30.7 and a best estimate of the threshold at 16 (Table 6). The gradient forest analysis provided further support for the second threshold, fully encompassing the estimated GAMM threshold range (Figure 12d).

Kyphosidae probability of presence increased with rugosity, peaking at values around 30 (deviance explained = 0.21, $p < 0.01$; Figure 11c). There were also two thresholds identified in this relationship. One ranged from 2.3 to 12.4, with the best estimate of the threshold location at a rugosity value of 7.3. The other threshold spanned values of 21.1 to 29.8, with a point estimate of 26.4 (Table 6). Both thresholds were additionally supported by the gradient forest analysis, with a gradient forest threshold overlapping the upper range of the first Kyphosidae GAMM threshold, and a second gradient forest threshold overlapping the second GAMM point estimate and upper threshold range (Figure 12d).

Chlorurus spilurus (uhu) exhibited an increase in probability of presence with increasing rugosity, with a slight intermediate peak at values around 20 (deviance explained = 0.25, $p < 0.01$; Figure 11d). *Chlorurus spilurus* (uhu) had four thresholds identified with rugosity. The first threshold ranged from 2.5 to 8.7, with the best estimate of the threshold location at 3.5. The second ranged from 10.7 to 23.7, with the best estimate at the rugosity value 18.2. The third threshold was estimated from 37.9 to 40.8, with the point estimate of 40.4, and the fourth threshold ranged from 48.3 to 50, with a point estimate of 50 (Table 6). The middle two thresholds were further supported by the gradient forest analysis, with the estimated threshold range fully encompassing the ranges of both GAMM estimated thresholds (Figure 12d).

Across all four binomial relationships, there were similar increasing trends but different overall shapes and magnitudes of relationships and threshold locations. All four indicators had a similar first threshold location for initial increases at rugosity values < 10, which might indicate the indicators share a response to the environmental feature (i.e., none inhabit flat seascapes). Again, the four indicators are not correlated with each other (Figures S1-S4) so we do not necessarily expect any similar relationships.

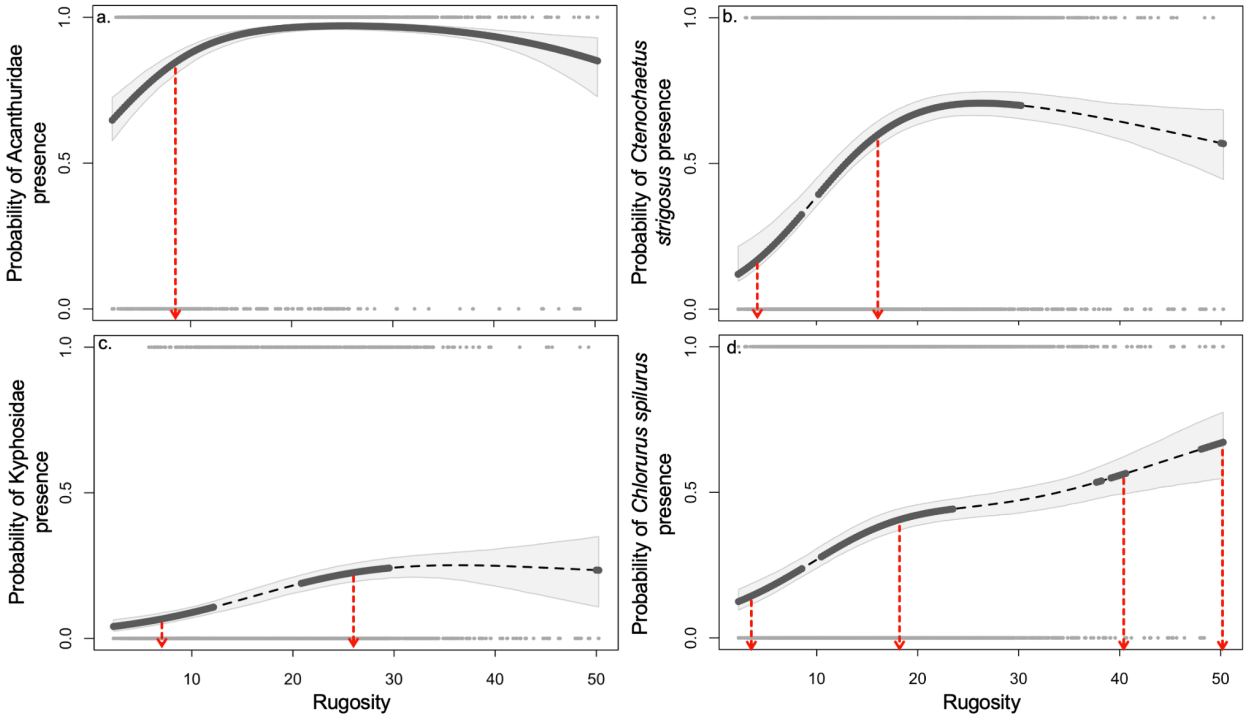

Figure 11. Fitted GAMMs for (a) the probability of family Acanthuridae presence, (b) the probability of *Ctenochaetus strigosus* (kole) presence, (c) the probability of family Kyphosidae, and (d) the probability of *Chlorurus spilurus* (uhu) presence with rugosity. The black dashed line is the GAMM smoothed function, the shaded interval represents the bootstrapped 95% confidence interval, and the gray points are the raw data. The bold line indicates the threshold range where the 95% CI of the second derivative does not include 0, while the dashed red lines show the best estimates for threshold locations (i.e., where the second derivative is most different from zero within the threshold range).

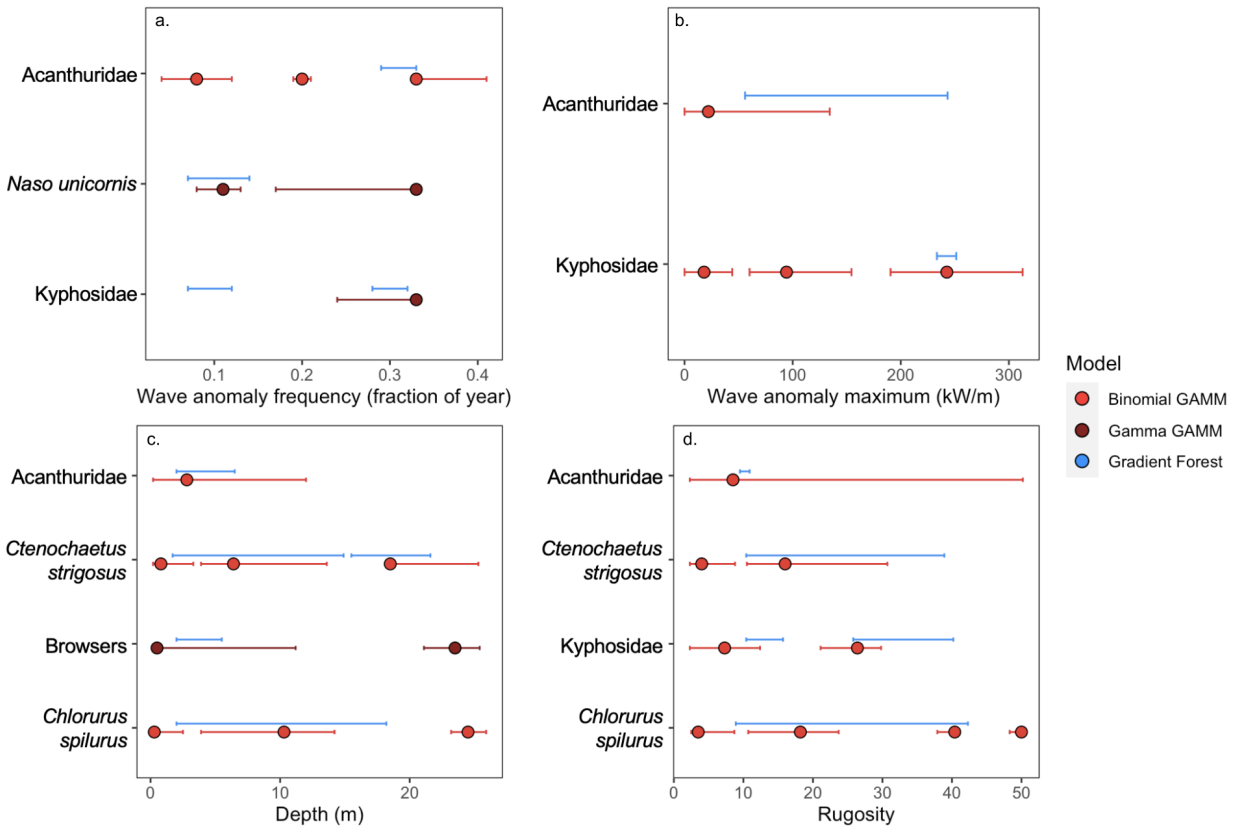

Figure 12. Comparison of identified thresholds across indicators and model types for (a) wave anomaly frequency, (b) wave anomaly maximum, (c) depth, and (d) rugosity. The binomially-distributed GAMM threshold ranges and point estimates are in red, the gamma-distributed GAMM threshold ranges and point estimates are in dark red, and the gradient forest threshold ranges are in blue.

Table 6. Nonlinear indicator-driver relationships that were supported by multi-model inference from the gradient forest and GAMM analyses, including location of threshold range(s), and the best estimate of threshold location(s). NTI = no threshold identified, '--' = information not determined from model.

Indicator	Driver / Pressure	Analysis	Location of threshold(s)	Best estimate of threshold location(s)
Acanthuridae	Wave anomaly frequency	Binomial GAMM	0.04 to 0.12	0.08
			0.19 to 0.21	0.2
			0.33 to 0.41	0.33
		Gradient Forest	0.29 to 0.33	--
	Wave anomaly maximum	Binomial GAMM	0 to 134.3	22
		Gradient Forest	55.9 to 243.3	--
	Depth	Binomial GAMM	0.2 to 12	2.8
		Gradient Forest	2 to 6.5	--
	Rugosity	Binomial GAMM	2.3 to 50.2	8.5
		Gradient Forest	9.5 to 10.9	--
Ctenochaetus strigosus	Depth	Binomial GAMM	0.2 to 3.3	0.8
			3.9 to 13.6	6.4
			18.5 to 25.3	18.5
		Gradient Forest	1.7 to 14.9	--
			15.5 to 21.6	--
	Rugosity	Binomial GAMM	2.3 to 8.8	4
			10.5 to 30.7	16
		Gradient Forest	10.4 to 38.9	--
Naso unicornis	Wave anomaly frequency	Gamma GAMM	0.08 to 0.13	0.11
			0.17 to 0.33	0.33
		Gradient Forest	0.07 to 0.14	--
Browsers	Depth	Gamma GAMM	0.3 to 11.2	0.5
			21.1 to 25.4	23.5
		Gradient Forest	2 to 5.5	--
Kyphosidae	Wave anomaly frequency	Gamma GAMM	0.24 to 0.33	0.33
		Gradient Forest	0.07 to 0.12	--
			0.28 to 0.32	--
	Wave anomaly maximum	Binomial GAMM	0 to 44.1	18
			60.1 to 154.4	94.3
			190.5 to 312.7	242.6
		Gamma GAMM	NTI	NTI
		Gradient Forest	233.4 to 251.3	--
	Rugosity	Binomial GAMM	2.3 to 12.4	7.3
			21.1 to 29.8	26.4
		Gradient Forest	10.4 to 15.7	--
			25.8 t0 40.2	--
Chlorurus spilurus	Depth	Binomial GAMM	0.29 to 2.5	0.29
			3.9 to 14.2	10.3
			23.2 to 25.9	24.5
		Gradient Forest	2 to 18.2	--
	Rugosity	Binomial GAMM	2.5 to 8.7	3.5
			10.7 to 23.7	18.2
			37.9 to 40.8	40.4
			48.3 to 50	50
		Gradient Forest	8.9 to 42.3	--

Discussion and Conclusions

Summary

We provided a step forward in the development of science that can support implementation of EBFM by exploring the potential for thresholds to be estimated for ecosystem indicators of Hawai‘i nearshore fisheries. Indicators can be useful for ecosystem-based approaches when they capture complex and dynamic ecosystem responses. We explored this utility by investigating whether there was evidence for commonalities in thresholds across species and their functional and family groups represented in nearshore fisheries in Hawai‘i. We found evidence for thresholds across four environmental drivers and multiple indicators, with some commonalities apparent, especially for habitat complexity (rugosity) and wave forcing. This represents a first step in assessing the utility of an indicator approach to EBFM for Pacific nearshore ecosystems.

Benefits and limitations of our approach

Several aspects of our approach were insightful and useful for progressing the science behind EBFM for nearshore Pacific ecosystems. We explored the existence of thresholds across a large set of environmental variables and found evidence for thresholds across four variables in particular: depth, habitat complexity (rugosity), and two metrics of wave forcing. These variables are all well known structuring variables for the ecology of nearshore tropical reefs (Dollar 1982, Wedding et al. 2011, 2013), and several of the common thresholds are relevant to the known ecologies of the indicators. For example, patterns for *Ctenochaetus strigosus* (kole) match our expectations based on the ecology of kole as detritivores that are associated with coral dominated areas with higher rugosity and intermediate depths (Randall 2010). Notably, peak kole presence occurred in similar depth and rugosity ranges as the modeled relationships of both drivers with Acanthuridae, suggesting a family-level trend that well-encompasses the ecology of the species nested within. Interestingly, several of the thresholds identified as common among indicators were from indicator pairs that were not correlated in the absence of the drivers, which provides evidence that these structuring variables are important for considering the ecosystem responses of the fisheries indicators we investigated. These conclusions are further supported by our approach that used multiple statistical models to assess the existence of threshold locations, with all of the threshold (ranges) identified by the gradient forest also supported by one or more GAMM threshold for each indicator-driver pair.

We also uncovered aspects of our approach that need further consideration for progressing the science behind EBFM. Many of the thresholds we identified occurred at either the minimum or maximum of the measured range of the driver, bringing to question the utility of these estimates. This was especially true when few values existed at either end of the driver range. One potential solution would be to consider a stricter cutoff for the overlap between the second derivative and zero, as most of the instances of thresholds at extreme driver values were associated with second derivatives that were barely above or below zero. Further, while there were many strengths to using multi-model inference to uncover potential ecosystem thresholds, there were also some downsides. Allowing for multiple opportunities to identify potential relationships may mean that one is uncovered when it may not have, but both gradient forests and GAMMs are

flexible approaches with a potential for overfitting, so a third more rigid framework could help differentiate important patterns from spurious ones. The Bayesian framework we described has the potential to fit this need, but we were unable to fit the models, potentially owing to the complexity of the relationships we studied. So, steps could be taken to add flexibility to the Bayesian framework while also maintaining the benefits it presents to assess the robustness of the threshold locations. We also separated the analyses of presence-absence and presence-only observations, which may limit our interpretations, because the two processes are linked and therefore it is not ecologically relevant to separate them. We did so to simplify the model forms since available tools for gradient forests and GAMMs are not available for models that fit the joint-probabilities (i.e., hurdle models). This is another potential advantage of continuing to explore the Bayseian framework, as incorporating joint-probabilities can be readily accomplished.

Management implications

This work serves as a step forward in developing science to support EBFM, but more work is needed to meet the broader objective to *provide a quantitative basis for ecosystem management that can be used to design effective management targets and measure and evaluate actions once they are in place*. Similar work in the California Current faced a similar conclusion, and suggested that this approach "may be particularly useful as a precautionary framework for identifying ecosystem components and relationships worthy of further detailed analyses" (Samhouri et al. 2017). Therefore we suggest that the six indicators and four drivers for which we identified potential threshold relationships can serve as a basis for further investigation of ecosystem trends.

We investigated multiple potential indicators for nearshore Hawai‘i ecosystems including both individual species and species complexes (taxonomic families and functional groups). In some cases we identified commonalities between the indicator-driver patterns for species and their associated complexes, and in other cases we found that patterns were different. For example, *Ctenochaetus strigosus* (kole) had similar patterns to Acanthuridae for depth and rugosity, but *Naso unicornis* (kala) had a very different pattern to Acanthuridae for wave anomaly frequency. Interestingly, most of the common thresholds we found were among species/groups that were not correlated with each other in the absence of the drivers. Given that many of the species that comprise nearshore fisheries in the Pacific are data poor, and when fisheries dependent data are collected they are often collected at the species complex level (e.g., all uhu combined in Hawai‘i), these results have implications for how these species might be monitored in relation to ecosystem-based management targets.

In addition to screening potential indicators and drivers for further analyses, this work also emphasizes the role of variation in environmental controls. We uncovered several common thresholds of environmental drivers across multiple indicators. While resource managers are not necessarily able to control environmental drivers like depth and wave forcing, understanding the limits of their control on ecosystem responses can provide a basis for monitoring and decision making. Data on nearshore reef fish populations is lacking for Pacific jurisdictions, while data on environmental drivers can potentially be easier to obtain through sources such as remote

sensing. Thus, knowing the threshold value for each driver in relation to EBFM indicators provides a potential mechanism to monitor indicator status indirectly. Further, understanding variation in environmental drivers over space and time could provide important context for management decisions, particularly given that human influences on ecosystems are often only possible to uncover once environmental variation has been accounted for (Williams et al. 2015).

Our analyses focused on environmental drivers rather than those associated with humans (e.g., fishing, land-based pollution) due to the importance of first understanding the role of environmental variation on indicators. Thus, future work can build on these to understand how humans alter those fundamental relationships. Considerations of scale are critical for effectively pairing environmental and human influences on ecosystem indicators (Donovan et al. 2022). For example, human drivers may influence ecosystem indicators at different scales, so the scale at which the driver is measured and modeled may influence the model's ability to uncover a relationship (Aston et al. 2019, Jouffray et al. 2019). Temporal matching is also critical, and often a challenging aspect of this work. For example, the environmental data we relied on was compiled for the Ocean Tipping Points project and was done so for a period representative of the data at the time the project occurred (2000-2013). While we were able to explore the option of updating the environmental driver layers (see interim reports), we made the decision to base our analyses on the earlier time period to align with previously conducted analyses (Friedlander et al. 2016, Donovan et al. 2018, Jouffray et al. 2019). Further, extreme temperatures that had large effects on marine ecosystems in Hawai‘i occurred in 2014-2015 (Kramer et al. 2016) and we did not have an effective means to incorporate those events without updated data on human drivers.

Next steps

Our exploration of the utility of multi-model inference to understand threshold relationships between indicators and drivers revealed several potential paths forward for continuing to advance the science of EBFM.

1. Improvements could be made to the implementation of the statistical methods that we explored. Principally, using Bayesian Hierarchical models (sensu Qian and Cuffney 2012) would have several advantages. First, it is a relatively stricter framework than gradient forests and GAMMs in that it is based on linear relationships with model selection against a null model, allowing for a robust check for the validity of the threshold (Qian 2014). Second, hurdle models that estimate the joint probabilities of presence-absence and biomass when present are more readily applied in a Bayesian framework. We were unable to fully explore these two advantages in the scope of this project, so they serve as promising pathways for next steps.
2. We focused our analyses on fished species associated with nearshore ecosystems in Hawai‘i given the relevance to EBFM applications. A potential interesting comparison could be to test for the existence of thresholds for non-fished species within the family and functional groups represented to both understand how the species complexes are representative of the species that comprise them, and evaluate the relative influence of fishing on the indicator groups.

3. Testing for the existence of thresholds in indicator-driver pairs across both environmental and human drivers will have more direct applications to EBFM. This will require appropriate data on drivers be generated at relevant temporal and spatial scales. Currently, available data is limited to pre-2013 (Lecky 2016, McCoy et al. 2018, Wedding et al. 2018). The project team is exploring possibilities for updating the data to more recent time periods outside of the scope of this project.
4. Understanding the role of climate change in altering relationships between indicators and drivers is critical given the increasing impact climate driven events are having on marine ecosystems (van Hooidonk et al. 2016, Hughes et al. 2017). In Hawai‘i, this is particularly relevant given the extreme temperatures that caused widespread coral bleaching events in 2014-15 and again in 2019 (Kramer et al. 2016, Winston et al. 2022).
5. Our analyses were focused on nearshore ecosystems in Hawai‘i as an initial step in developing science to support implementation of EBFM for nearshore reef ecosystems in the Pacific. The focus on Hawai‘i was largely due to the availability of data on indicators from the Hawai‘i Monitoring and Reporting Collaborative (Donovan et al. 2020). Similar efforts to compile existing monitoring datasets in other jurisdictions could enable similar analyses to be conducted in those ecosystems.

Acknowledgements

This work would not have been possible without the generous contributions of the data providers of the Hawaii Monitoring and Reporting Collaborative: the Hawai‘i Division of Aquatic Resources (DAR), the Coral Reef Assessment and Monitoring Program (CRAMP), the Fisheries Ecology Research Laboratory (FERL) at the University of Hawai‘i (UH), the National Oceanic and Atmospheric Administration (NOAA) National Coral Reef Monitoring Program, the National Parks Service (NPS) Inventory and Monitoring Program, and The Nature Conservancy (TNC). We also thank Jameal Samhouri and Mary Hunsicker for help with scoping the original project ideas and lending their encouragement from their work in the California Current. We are also grateful to Joey Lecky for his work to create and maintain the driver databases that made this work possible, and to Chelsie Counsell and Megan Donahue for their contributions to the maintenance of the HIMARC database. Funding for this project was provided by the Western Pacific Regional Fishery Management Council through its cooperative agreement with the NOAA Coral Reef Conservation Program (Award No. NA20NMF4410262).

Literature Cited

Arkema, K. K., S. C. Abramson, and B. M. Dewsbury. 2006. Marine ecosystem-based management: from characterization to implementation. Frontiers in ecology and the environment 4:525–532.

Aston, E. A., G. J. Williams, J. A. M. Green, A. J. Davies, L. M. Wedding, J. M. Gove, J. Jouffray, T. T. Jones, and J. Clark. 2019. Scale‐dependent spatial patterns in benthic communities around a tropical island seascape. Ecography 42:578–590.

Boldt, J. L., R. Martone, J. Samhouri, R. I. Perry, S. Itoh, I. K. Chung, M. Takahashi, and N. Yoshie. 2014. Ecosystem Indicators for Responses to Multiple Stressors. Oceanography 27:116–116.

Carpenter, Gelman, Hoffman, and Lee. 2017. Stan: A probabilistic programming language. Journal of statistical and econometric methods.

Crowder, L., and E. Norse. 2008. Essential ecological insights for marine ecosystem-based management and marine spatial planning. Marine Policy 32:772–778.

DeMartini, E. E., and K. G. Howard. 2016. Comparisons of body sizes at sexual maturity and at sex change in the parrotfishes of Hawaii: input needed for management regulations and stock assessments. Journal of fish biology.

Dolan, T. E., W. S. Patrick, and J. S. Link. 2015. Delineating the continuum of marine ecosystem-based management: a US fisheries reference point perspective. ICES journal of marine science: journal du conseil 73:1042–1050.

Dollar, S. J. 1982. Wave stress and coral community structure in Hawaii. Coral reefs 1:71–81.

Dollar, S. J., and R. W. Grigg. 2004. Anthropogenic and natural stresses on selected coral reefs in Hawai'i: A multidecade synthesis of impact and recovery. Pacific science 58:281–304.

Donovan, M. K., C. Alves, J. Burns, C. Drury, O. W. Meier, R. Ritson-Williams, R. Cunning, R. P. Dunn, G. Goodbody-Gringley, L. M. Henderson, I. S. S. Knapp, J. Levy, C. A. Logan, L. Mudge, C. Sullivan, R. D. Gates, and G. P. Asner. 2022. From polyps to pixels: understanding coral reef resilience to local and global change across scales. Landscape ecology.

Donovan, M. K., C. W. W. Counsell, J. Lecky, and M. J. Donahue. 2020. Estimating indicators and reference points in support of effectively managing nearshore marine resources in Hawai‘i.

Donovan, M. K., A. M. Friedlander, J. Lecky, J. B. Jouffray, G. J. Williams, L. M. Wedding, L. B. Crowder, A. L. Erickson, N. A. J. Graham, J. M. Gove, C. V. Kappel, K. Karr, J. N. Kittinger, A. V. Norström, M. Nyström, K. L. L. Oleson, K. A. Stamoulis, C. White, I. D. Williams, and K. A. Selkoe. 2018. Combining fish and benthic communities into multiple regimes reveals complex reef dynamics. Scientific reports 8.

Ellis, N., S. J. Smith, and C. R. Pitcher. 2012. Gradient forests: calculating importance gradients on physical predictors. Ecology 93:156–168.

Foley, M. M., M. H. Armsby, E. E. Prahler, M. R. Caldwell, A. L. Erickson, J. N. Kittinger, L. B. Crowder, and P. S. Levin. 2013. Improving ocean management through the use of ecological principles and integrated ecosystem assessments. Bioscience 63:619–631.

Foley, M. M., R. G. Martone, M. D. Fox, C. V. Kappel, L. A. Mease, A. L. Erickson, B. S. Halpern, K. A. Selkoe, P. Taylor, and C. Scarborough. 2015. Using ecological thresholds to

inform resource management: current options and future possibilities. Frontiers in Marine Science 2:95–95.
Friedlander, A. M., E. E. Brown, P. I. Jokiel, W. R. Smith, and K. S. Rodgers. 2003. Effects of habitat, wave exposure, and marine protected area status on coral reef fish assemblages in the Hawaiian Archipelago. Coral reefs 22:291–305.
Friedlander, A. M., and E. E. DeMartini. 2002. Contrasts in density, size, and biomass of reef fishes between the northwestern and the main Hawaiian islands: the effects of fishing down apex predators. Marine ecology progress series 230:253–264.
Friedlander, A. M., M. K. Donovan, K. Stamoulis, and I. D. Williams. 2016. Contemporary human impacts on coral reef fishes through the lens of customary fisheries management boundaries in Hawaii. PloS one:In review–In review.
Gelman, A., J. B. Carlin, H. S. Stern, D. B. Dunson, A. Vehtari, and D. B. Rubin. 2013. Bayesian data analysis. CRC press.
Gove, J. M., G. J. Williams, M. A. McManus, S. F. Heron, S. A. Sandin, O. J. Vetter, and D. G. Foley. 2013. Quantifying climatological ranges and anomalies for Pacific coral reef ecosystems. PloS one 8.
Grigg, R. W. 1998. Holocene coral reef accretion in Hawaii: A function of wave exposure and sea level history. Coral reefs 17:263–272.
Halpern, B. S., C. V. Kappel, K. A. Selkoe, F. Micheli, C. M. Ebert, C. Kontgis, C. M. Crain, R. G. Martone, C. Shearer, and S. J. Teck. 2009. Mapping cumulative human impacts to California Current marine ecosystems. Conservation letters 2:138–148.
Harvey, C. J., C. R. Kelble, and F. B. Schwing. 2016. Implementing “the IEA”: using integrated ecosystem assessment frameworks, programs, and applications in support of operationalizing ecosystem-based management. ICES journal of marine science: journal du conseil 74:398–405.
van Hooidonk, R., J. Maynard, J. Tamelander, J. Gove, G. Ahmadia, L. Raymundo, G. Williams, S. F. Heron, and S. Planes. 2016. Local-scale projections of coral reef futures and implications of the Paris Agreement. Scientific reports 6:39666–39666.
Hughes, T. P., M. L. Barnes, D. R. Bellwood, J. E. Cinner, G. S. Cumming, J. B. C. Jackson, J. Kleypas, I. A. van de Leemput, J. M. Lough, T. H. Morrison, S. R. Palumbi, E. H. van Nes, and M. Scheffer. 2017. Coral reefs in the Anthropocene. Nature 546:82–90.
Hunsicker, M. E., C. V. Kappel, K. A. Selkoe, B. S. Halpern, C. Scarborough, L. Mease, and A. Amrhein. 2016. Characterizing driver–response relationships in marine pelagic ecosystems for improved ocean management. Ecological applications: a publication of the Ecological Society of America 26:651–663.
Jokiel, P. L., E. K. Brown, A. Friedlander, S. K. Rodgers, and W. R. Smith. 2004. Hawai’i coral reef assessment and monitoring program: Spatial patterns and temporal dynamics in reef coral communities. Pacific science 58:159–174.
Jouffray, J.-B., L. M. Wedding, A. V. Norström, M. K. Donovan, G. J. Williams, L. B. Crowder, A. L. Erickson, A. M. Friedlander, N. A. J. Graham, J. M. Gove, C. V. Kappel, J. N. Kittinger, J. Lecky, K. L. L. Oleson, K. A. Selkoe, C. White, I. D. Williams, and M. Nyström. 2019. Parsing human and biophysical drivers of coral reef regimes. Proceedings of the Royal Society B: Biological Sciences 286.
Kramer, K., S. Cotton, M. Lamson, and W. Walsh. 2016. Bleaching and catastrophic mortality of

reef-building corals along west Hawai ‘i island: findings and future directions. Pages 229–241.
Large, S. I., G. Fay, K. D. Friedland, and J. S. Link. 2013. Defining trends and thresholds in responses of ecological indicators to fishing and environmental pressures. ICES journal of marine science: journal du conseil 70:755–767.
Large, S. I., G. Fay, K. D. Friedland, and J. S. Link. 2015. Quantifying patterns of change in marine ecosystem response to multiple pressures. PloS one 10:e0119922–e0119922.
Lecky, J. 2016. Ecosystem vulnerability and mapping cumulative impacts on Hawaiian reefs.
Lester, S. E., C. Costello, B. S. Halpern, S. D. Gaines, C. White, and J. A. Barth. 2013. Evaluating tradeoffs among ecosystem services to inform marine spatial planning. Marine Policy 38:80–89.
Levin, P. S., M. J. Fogarty, S. A. Murawski, and D. Fluharty. 2009. Integrated ecosystem assessments: developing the scientific basis for ecosystem-based management of the ocean. PLoS biology 7:e1000014–e1000014.
Levin, S. A., and J. Lubchenco. 2008. Marine ecosystem-based management. Bioscience 58:1–7.
Link, J. S. 2005. Translating ecosystem indicators into decision criteria. ICES journal of marine science: journal du conseil 62:569–576.
McCoy, K. S., I. D. Williams, A. M. Friedlander, H. Ma, L. Teneva, and J. N. Kittinger. 2018. Estimating nearshore coral reef-associated fisheries production from the main Hawaiian Islands. PloS one 13:e0195840–e0195840.
Mcleod, K., and H. Leslie, editors. 2009. Ecosystem-based management for the oceans. Island Press, Washington D.C.
Methratta, E., and J. Link. 2006. Evaluation of quantitative indicators for marine fish communities. Ecological indicators 6:575–588.
Nadon, M. O., J. S. Ault, I. D. Williams, S. G. Smith, and G. T. DiNardo. 2015. Length-Based Assessment of Coral Reef Fish Populations in the Main and Northwestern Hawaiian Islands. PloS one 10:e0133960–e0133960.
Plummer, M. 2016. rjags: Bayesian Graphical Models using MCMC. R package version 4-6. https://CRAN.R-project.org/package=rjags.
Qian, S. S. 2014. Ecological threshold and environmental management: A note on statistical methods for detecting thresholds. Ecological indicators 38:192–197.
Qian, S. S., and T. F. Cuffney. 2012. To threshold or not to threshold? That’s the question. Ecological indicators 15:1–9.
Randall, J. E. 2010. Shore Fishes of Hawaii: Revised Edition. University of Hawaii Press.
Samhouri, J. F., K. S. Andrews, G. Fay, C. J. Harvey, E. L. Hazen, S. M. Hennessey, K. Holsman, M. E. Hunsicker, S. I. Large, K. N. Marshall, A. C. Stier, J. C. Tam, and S. G. Zador. 2017. Defining ecosystem thresholds for human activities and environmental pressures in the California Current. Ecosphere 8:e01860.
Samhouri, J. F., A. J. Haupt, P. S. Levin, J. S. Link, and R. Shuford. 2013. Lessons learned from developing integrated ecosystem assessments to inform marine ecosystem-based management in the USA. ICES journal of marine science: journal du conseil:fst141–fst141.
Samhouri, J. F., P. S. Levin, and C. H. Ainsworth. 2010. Identifying thresholds for ecosystem-based management. PloS one 5:e8907–e8907.

Samhouri, J. F., P. S. Levin, and C. J. Harvey. 2009. Quantitative evaluation of marine ecosystem indicator performance using food web models. Ecosystems 12:1283–1298.

Selkoe, K. A., T. Blenckner, M. R. Caldwell, L. B. Crowder, A. L. Erickson, T. E. Essington, J. A. Estes, R. M. Fujita, B. S. Halpern, and M. E. Hunsicker. 2015. Principles for managing marine ecosystems prone to tipping points. Ecosystem Health and Sustainability 1:1–18.

Tam, J. C., J. S. Link, S. I. Large, K. Andrews, K. D. Friedland, J. Gove, E. Hazen, K. Holsman, M. Karnauskas, and J. F. Samhouri. 2017. Comparing apples to oranges: common trends and thresholds in anthropogenic and environmental pressures across multiple marine ecosystems. Frontiers in Marine Science 4:282–282.

The California Current Integrated Ecosystem Assessment: Phase III Report. 2014. . Page Available from http://www.noaa.gov/iea/CCIEA–Repor.

Wedding, L. M., J. Lecky, J. M. Gove, H. Walecka, M. K. Donovan, G. J. Williams, J. Jouffray, L. B. Crowder, A. L. Erickson, K. Falinski, A. M. Friedlander, C. V. Kappel, J. N. Kittinger, K. McCoy, A. V. Norström, M. Nyström, K. L. L. Oleson, K. A. Stamoulis, C. White, and K. A. Selkoe. 2018. Advancing the Integration of Spatial Data to Map Human and Natural Drivers on Coral Reefs. PloS one in press.

Wedding, L. M., C. A. Lepczyk, S. J. Pittman, A. M. Friedlander, and S. Jorgensen. 2011. Quantifying seascape structure: extending terrestrial spatial pattern metrics to the marine realm. Marine ecology progress series 427:219–232.

White, C., B. S. Halpern, and C. V. Kappel. 2012. Ecosystem service tradeoff analysis reveals the value of marine spatial planning for multiple ocean uses. Proceedings of the National Academy of Sciences 109:4696–4701.

Williams, G. J., J. M. Gove, Y. Eynaud, B. J. Zgliczysnki, and S. A. Sandin. 2015. Local human impacts decouple natural biophysical relationships on Pacific coral reefs. Ecography 38:1–11.

Williams, I. D., W. J. Walsh, R. E. Schroeder, A. M. Friedlander, B. L. Richards, and K. A. Stamoulis. 2008. Assessing the importance of fishing impacts on Hawaiian coral reef fish assemblages along regional-scale human population gradients. Environmental conservation 35:261–261.

Winston, M., T. Oliver, C. Couch, M. K. Donovan, G. P. Asner, E. Conklin, K. Fuller, B. W. Grady, B. Huntington, K. Kageyama, T. L. Kindinger, K. Kozar, L. Kramer, T. Martinez, A. McCutcheon, S. McKenna, K. ’ulei Rodgers, C. K. Shayler, B. Vargas-Angel, and B. Zgliczynski. 2022. Coral taxonomy and local stressors drive bleaching prevalence across the Hawaiian Archipelago in 2019. PloS one 17:e0269068.

Zuur, A. F., J. M. Hilbe, and E. N. Ieno. 2013. A Beginner’s Guide to GLM and GLMM with R: A Frequentist and Bayesian Perspective for Ecologists. Highland Statistics Limited.

Appendix

Correlations among the species, species complexes, and functional groups

With our indicator species, species complexes, and functional groups selected, we first evaluated correlations between fish groups. Because our analyses hinge upon fish biomass from several nested groupings (species within species complexes, and species within functional groups), this helps inform the interpretations of our subsequent models and the identified threshold relationships. Thus, Pearson's correlations were calculated for each species and species complex (Figure S1) and functional group pairings (Figure S2) to determine correlations in biomass between candidate indicator species and the species complexes and functional groups the species are nested within.

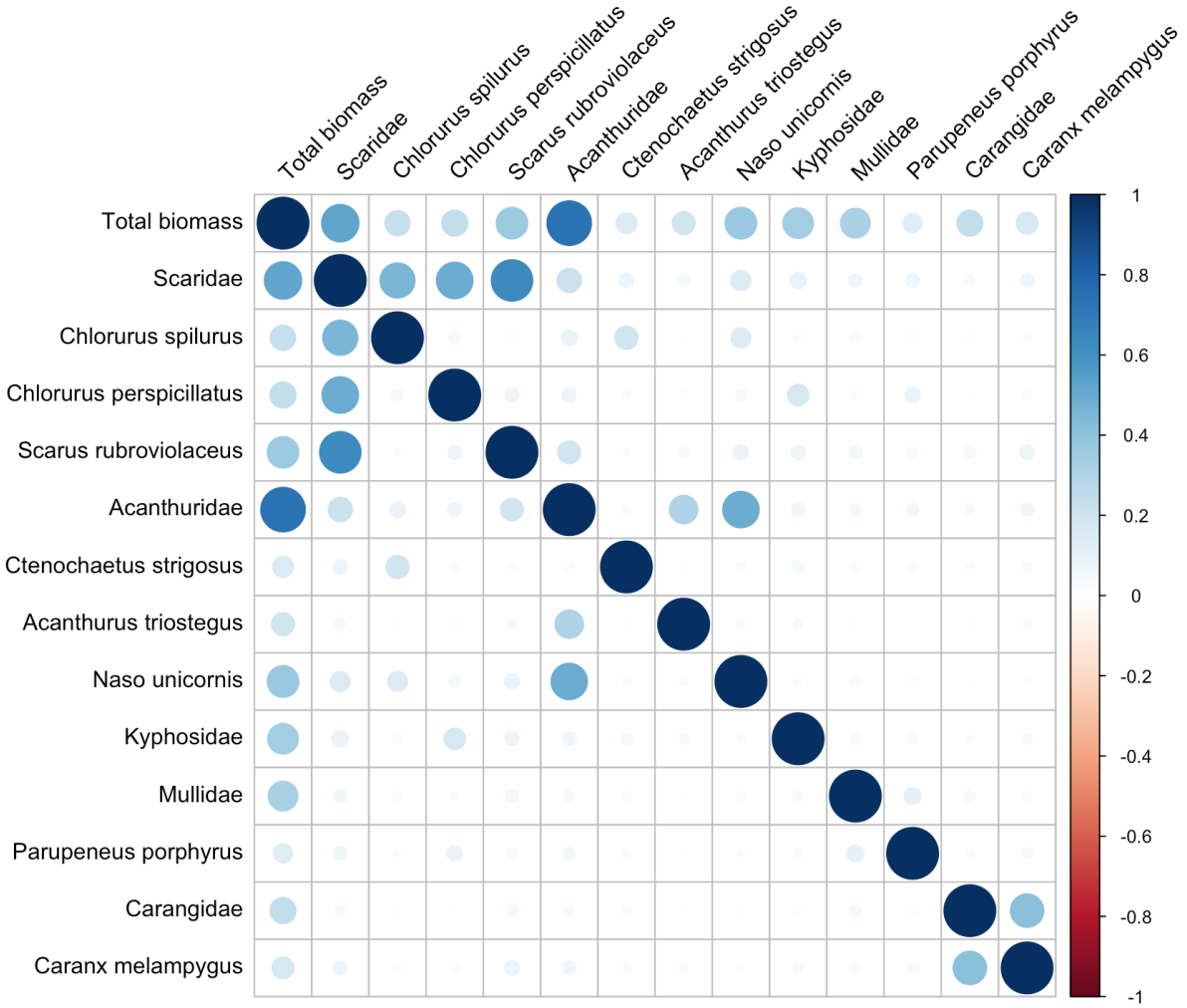

Figure S1. Pearson's correlations between species and family (species complex) biomass. Darker colors indicate stronger correlations.

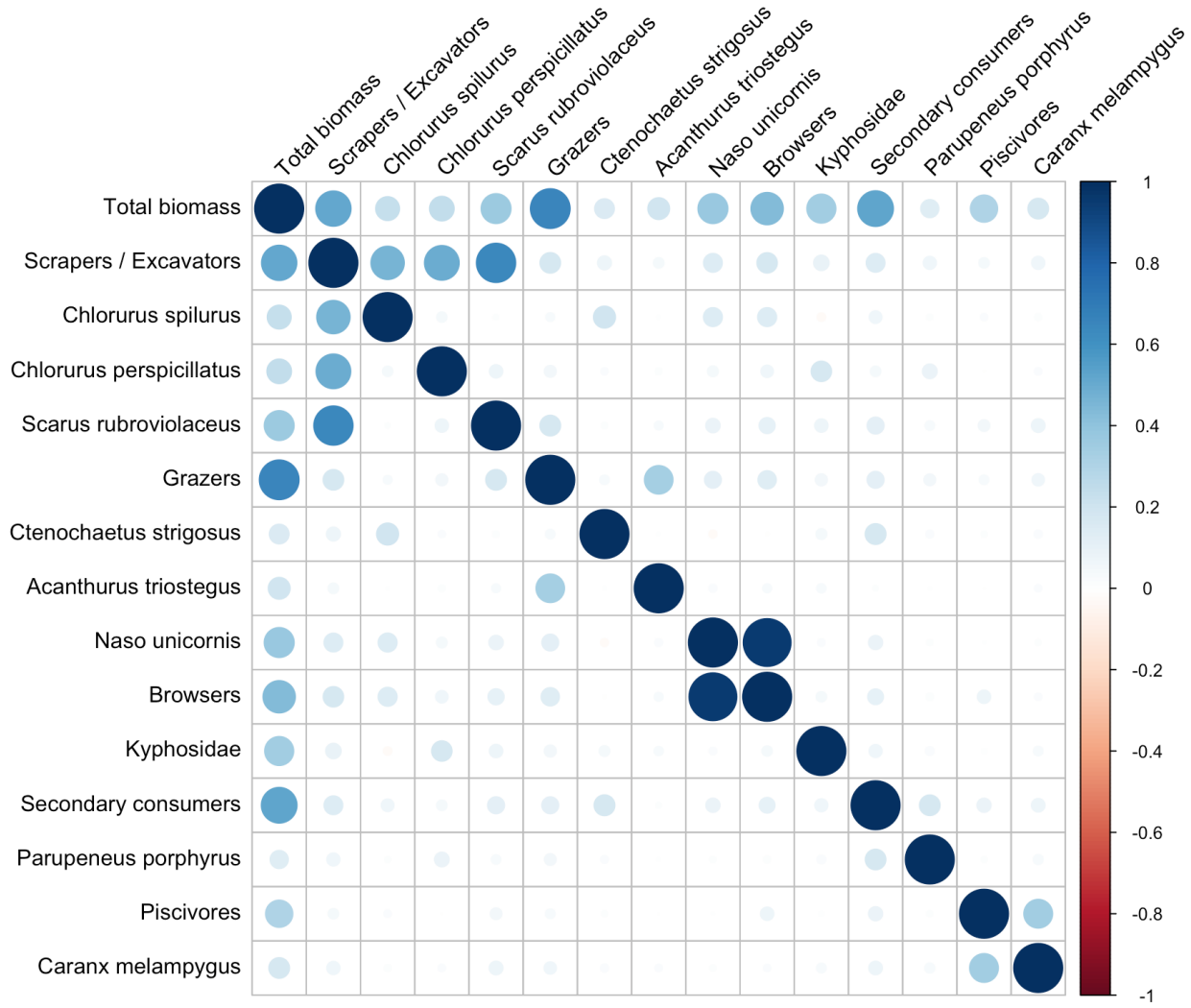

Figure S2. Pearson's correlations between species and functional group biomass. Darker colors indicate stronger correlations.

Most species, species complexes, and functional groups were positively correlated with total fish biomass, but the strength of species-level correlations varied both across and within species complexes (Figures S1 and S2). Correlations ranged between 0 and 0.95, indicating that the utility of family and functional group biomass to describe species dynamics varies. We considered a correlation coefficient of greater than 0.2 or 0.45 to indicate a moderate or strong correlation, respectively.

The species nested within the family Scaridae were highly correlated with family-level biomass (*Chlorurus spilurus* Pearson's r = 0.46, *Chlorurus perspicillatus* Pearson's r = 0.50, *Scarus rubroviolaceus* Pearson's r = 0.64; Figures S3b,e,h) and moderately correlated with total fish biomass (*C. spilurus* Pearson's r = 0.23, *C. perspicillatus* Pearson's r = 0.25, *S. rubroviolaceus* Pearson's r = 0.37; Figures S3a,d,g), but not with each other (Figure S1). These species were also highly correlated with the scraper/excavator functional group biomass (*C. spilurus*

Pearson's r = 0.46, *C. perspicillatus* Pearson's r = 0.50, *S. rubroviolaceus* Pearson's r = 0.64; Figures S3c,f,i), suggesting that these large bodied scarids are important contributors to overall biomass within that functional group.

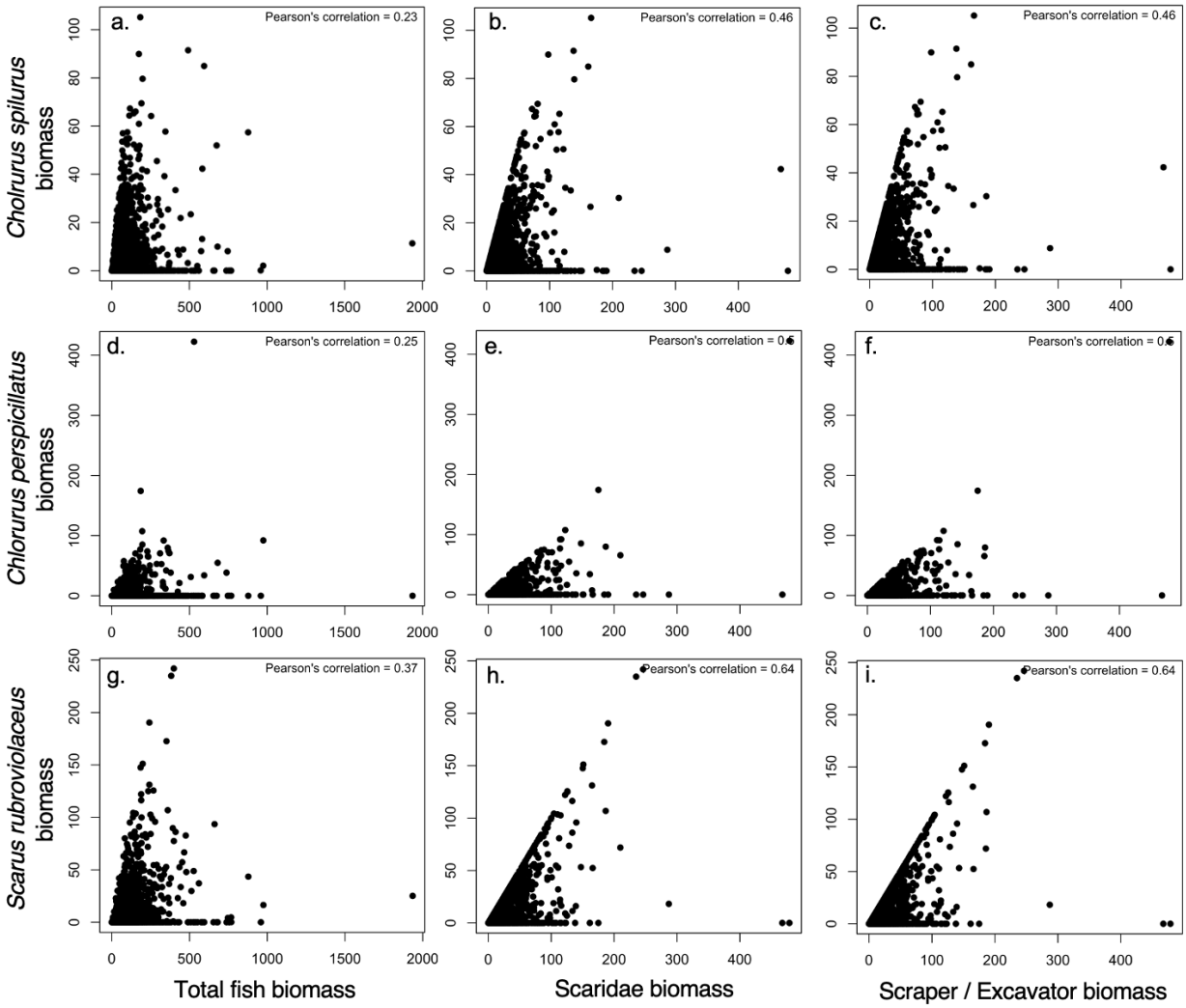

Figure S3. Correlations between Fisheries Local Action Strategy in Hawai'i (FLASH) priority species in the family Scaridae and (a,d,g) total fish biomass, (b,e,h) species complex biomass, and (c,f,i) functional group biomass.

Species nested within the family Acanthuridae showed varied correlation strengths with total fish biomass, species complex biomass, and functional group biomass (Figures S1, S2, S4). *Naso unicornis* (kala) was highly correlated with its species complex biomass (Pearson's r = 0.49; Figures S1, S4b), as well as browser biomass (Pearson's r = 0.95; Figures S2, S4c). However, both *Ctenochaetus strigosus* (kole) and *Acanthurus triostegus* (manini)did not exhibit strong correlations to either their species complex biomass (*C. strigosus* Pearson's r = 0.03, *A. triostegus* Pearson's r = 0.28; Figures S2, S4e,h) or functional group biomass (*C. strigosus* Pearson's r = 0.04, *A. triostegus* Pearson's r = 0.30; Figures S2, S4f,i). The lack of correlations

for manini and kole may be due to either the large numbers of samples with no fish present or the potential for these species to school in large aggregations.

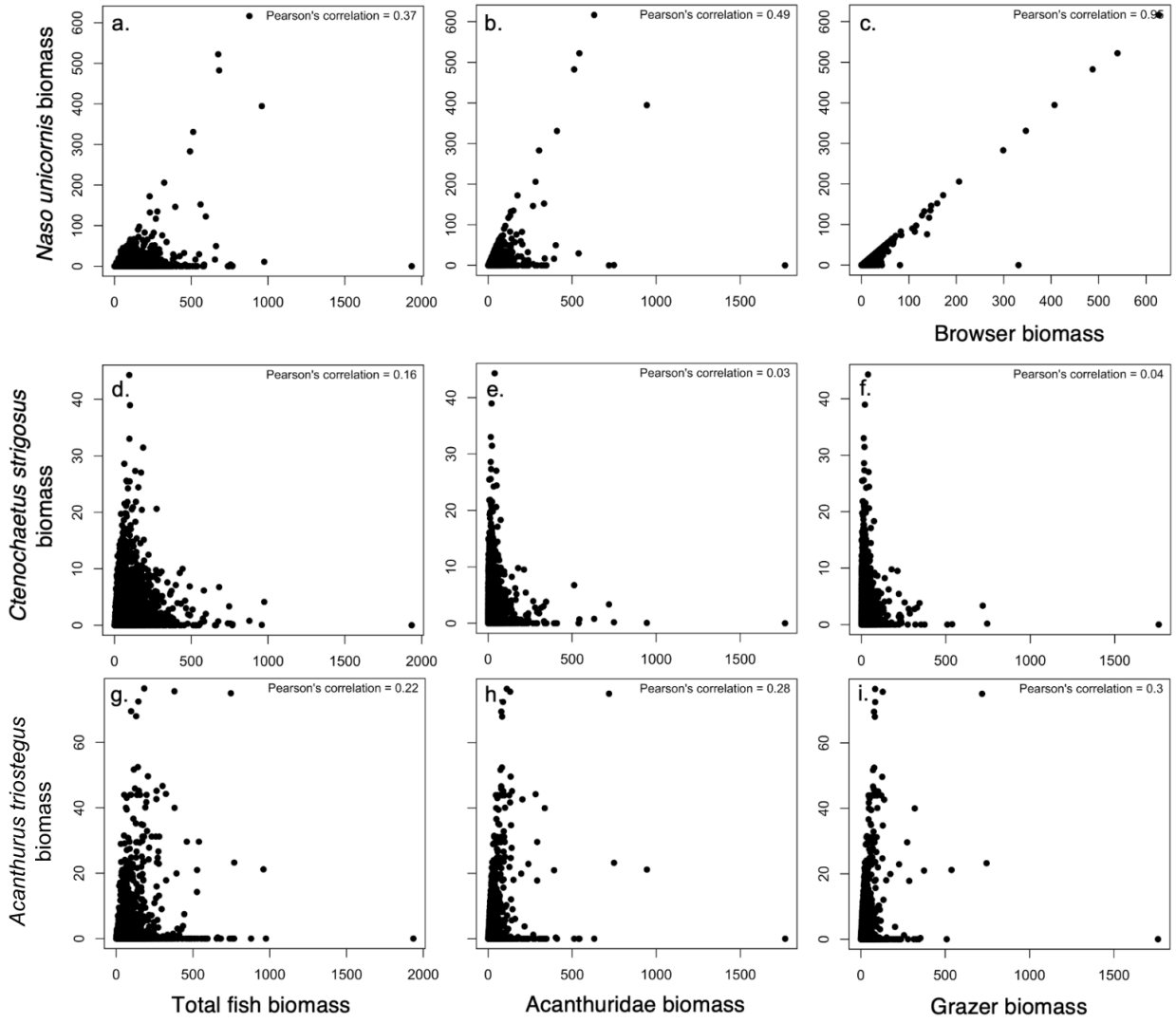

Figure S4. Correlations between Fisheries Local Action Strategy in Hawai'i (FLASH) priority species in the family Acanthuridae and (a,d,g) total fish biomass, (b,e,h) species complex biomass, and (c,f,i) functional group biomass.

Species in the family Mullidae exhibited weak correlations with total fish biomass and species complex biomass (*Parupeneus porphyrus* Pearson's r = 0.13 and 0.10, respectively; Figures S1, S5a,b), as well as secondary consumer biomass (*P. porphyrus* Pearson's r = 0.17; Figures S2, S5c). However, species in the family Carangidae showed moderate correlations with species complex biomass (*Caranx melampygus* Pearson's r = 0.41; Figures S1, S6b) as well as piscivore biomass (*C. melampygus* Pearson's r = 0.34; Figures S2, S6c).

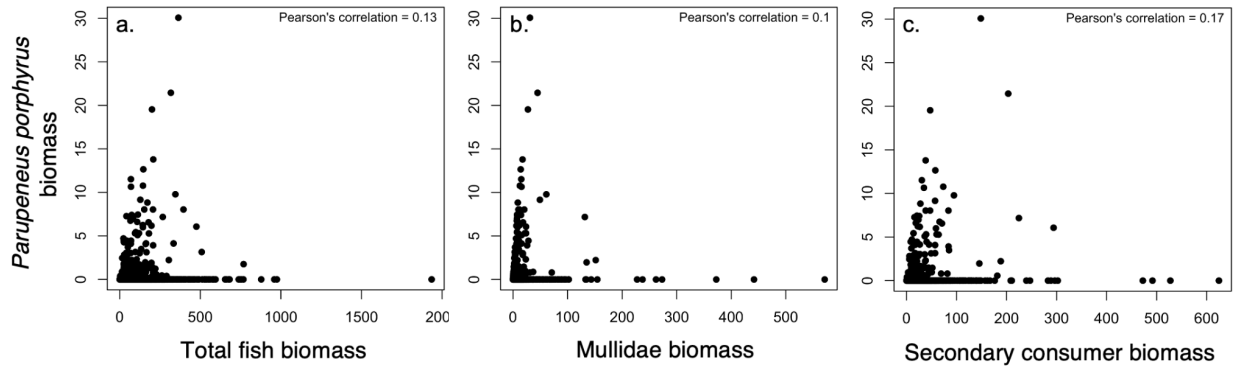

Figure S5. Correlations between Fisheries Local Action Strategy in Hawai‘i (FLASH) priority species in the family Mullidae and (a) total fish biomass, (b) species complex biomass, and (c) functional group biomass.

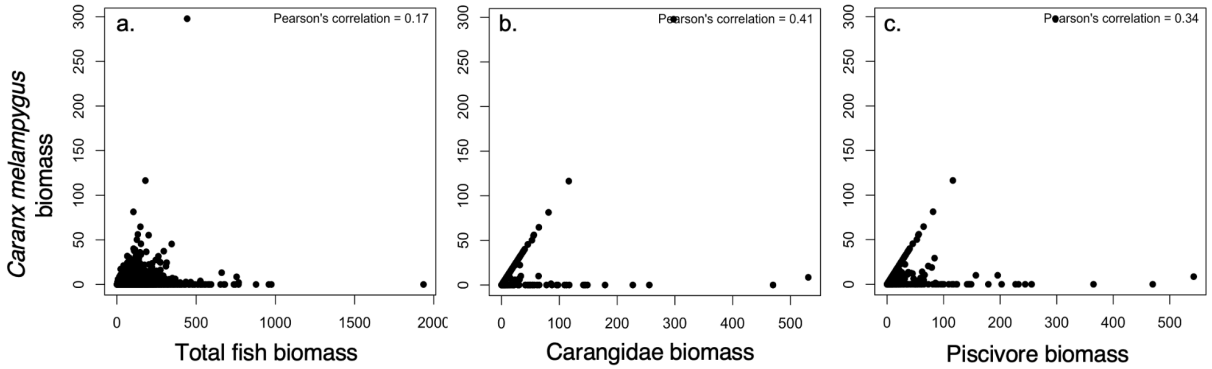

Figure S6. Correlations between Fisheries Local Action Strategy in Hawai‘i (FLASH) priority species in the family Carangidae and (a) total fish biomass, (b) species complex biomass, and (c) functional group biomass.